



10-2014

The Role of Th-U Minerals in Assessing the Performance of Nuclear Waste Forms

Gregory R. Lumpkin

Yan Gao

Reto Gieré


University of Pennsylvania, gier@sas.upenn.edu

C T. Williams

Anthony Mariano

See next page for additional authors

Follow this and additional works at: http://repository.upenn.edu/ees_papers

 Part of the [Geology Commons](#), and the [Mineral Physics Commons](#)

Recommended Citation

Lumpkin, G. R., Gao, Y., Gieré, R., Williams, C. T., Mariano, A., & Geisler, T. (2014). The Role of Th-U Minerals in Assessing the Performance of Nuclear Waste Forms. *Mineralogical Magazine*, 78 (5), 1071-1095. <http://dx.doi.org/10.1180/minmag.2014.078.5.01>

At the time of publication, author Reto Gieré was affiliated with the Institute of Earth and Environmental Sciences Geochemistry, University of Freiburg. Currently, he is a faculty member in the Earth & Environmental Science Department at the University of Pennsylvania.

This paper is posted at ScholarlyCommons. http://repository.upenn.edu/ees_papers/98

For more information, please contact repository@pobox.upenn.edu.

The Role of Th-U Minerals in Assessing the Performance of Nuclear Waste Forms

Abstract

Materials designed for nuclear waste disposal include a range of ceramics, glass ceramics and glass waste forms. Those with crystalline phases have provided the momentum for studies of minerals as a means to understand aspects of waste-form crystal chemistry, behaviour in aqueous systems and radiation damage over geological periods of time. Although the utility of natural analogue studies varies, depending upon the degree of analogy to the proposed geological repository and other factors such as chemical composition, the available data suggest that Th-U host phases such as brannerite, monazite, pyrochlore, zircon and zirconolite are resistant generally to dissolution in aqueous fluids at low temperatures. Geochemical durability may or may not extend to hydrothermal systems depending on the specifics of fluid composition, temperature and pressure. At elevated temperatures, for example, davidite may break down to new phase assemblages including titanite, ilmenite and rutile. Perovskite is generally less resistant to dissolution at low temperatures and breaks down to TiO₂, releasing A-site cations to the aqueous fluid. Studies of radiation damage indicate that the oxide and silicate phases become amorphous as a result of the gradual accumulation of alpha-recoil collision cascades. Monazite tends to remain crystalline on geological time scales, a very attractive property that potentially eliminates major changes in physical properties such as density and volume, thereby reducing the potential for cracking, which is a major concern for zircon. In spite of recent success in describing the behaviour of Th-U minerals in geological systems, considerable work remains in order to understand the *P-T-X* conditions during alteration and *T-t* history of the host rocks.

Keywords

actinides, brannerite, carbonatite, davidite, granitic pegmatite, hydrothermal veins, monazite, nuclear waste, perovskite, pyrochlore, thorium, uranium, zircon, zirconolite

Disciplines

Geology | Mineral Physics

Comments

At the time of publication, author Reto Gieré was affiliated with the Institute of Earth and Environmental Sciences Geochemistry, University of Freiburg. Currently, he is a faculty member in the Earth & Environmental Science Department at the University of Pennsylvania.

Author(s)

Gregory R. Lumpkin, Yan Gao, Reto Gieré, C T. Williams, Anthony Mariano, and Thorsten Geisler

The role of Th-U minerals in assessing the performance of nuclear waste forms

G. R. LUMPKIN^{1,*}, YAN GAO¹, R. GIERÉ², C. T. WILLIAMS³, A. N. MARIANO⁴ AND T. GEISLER⁵

¹ Institute of Materials Engineering, Australian Nuclear Science and Technology Organisation, Locked Bag 2001, Kirrawee DC, NSW 2232, Australia

² Institute of Earth and Environmental Sciences Geochemistry, University of Freiburg, Albertstrasse 23-B, Freiburg, D-79104, Germany

³ Department of Mineralogy, The Natural History Museum, Cromwell Road, London SW7 5BD, UK

⁴ 48 Page Brook Road, Carlisle, MA 10741, Massachusetts, USA

⁵ Steinmann Institute, University of Bonn, Bonn, D-53012, Germany

[Received 7 December 2013; Accepted 12 June 2014; Associate Editor: A. Pring]

ABSTRACT

Materials designed for nuclear waste disposal include a range of ceramics, glass ceramics and glass waste forms. Those with crystalline phases have provided the momentum for studies of minerals as a means to understand aspects of waste-form crystal chemistry, behaviour in aqueous systems and radiation damage over geological periods of time. Although the utility of natural analogue studies varies, depending upon the degree of analogy to the proposed geological repository and other factors such as chemical composition, the available data suggest that Th-U host phases such as brannerite, monazite, pyrochlore, zircon and zirconolite are resistant generally to dissolution in aqueous fluids at low temperatures. Geochemical durability may or may not extend to hydrothermal systems depending on the specifics of fluid composition, temperature and pressure. At elevated temperatures, for example, davidite may break down to new phase assemblages including titanite, ilmenite and rutile. Perovskite is generally less resistant to dissolution at low temperatures and breaks down to TiO₂, releasing A-site cations to the aqueous fluid. Studies of radiation damage indicate that the oxide and silicate phases become amorphous as a result of the gradual accumulation of alpha-recoil collision cascades. Monazite tends to remain crystalline on geological time scales, a very attractive property that potentially eliminates major changes in physical properties such as density and volume, thereby reducing the potential for cracking, which is a major concern for zircon. In spite of recent success in describing the behaviour of Th-U minerals in geological systems, considerable work remains in order to understand the *P-T-X* conditions during alteration and *T-t* history of the host rocks.

KEYWORDS: actinides, brannerite, carbonatite, davidite, granitic pegmatite, hydrothermal veins, monazite, nuclear waste, perovskite, pyrochlore, thorium, uranium, zircon, zirconolite.

Introduction

AFTER ~50 years of commercial nuclear energy production, substantial quantities of nuclear waste materials continue to be stored in temporary facilities while awaiting the development of

geological repositories. As the spent nuclear fuel from commercial power reactors continues to

This paper is published as part of a special set in *Mineralogical Magazine*, Volume 78(5), 2014, entitled 'GEOLIFE—Geomaterials for the environment, technology and human activities' arising out of papers presented at the Goldschmidt 2013 conference.

* E-mail: grl@ansto.gov.au

DOI: 10.1180/minmag.2014.078.5.01

accumulate, several countries are also attempting to come to terms with ‘legacy’ nuclear materials derived from the developmental era of nuclear power, the production of weapons during the Cold War period and other activities involving nuclear materials. The main options for the long-term storage or disposal of unusable nuclear materials are direct disposal of spent fuel, vitrification of wastes in borosilicate glass, or encapsulation of a range of materials in ceramic and glass-ceramic waste forms. A number of countries including Canada, Finland, Spain, Sweden and the United States have adopted a once-through nuclear fuel cycle with direct disposal of spent fuel as the chosen option. Others such as Belgium, China, France, India, Japan, Russia and the United Kingdom rely on multiple cycles of fuel usage with reprocessing steps, thereby generating high-level nuclear waste (HLW) that must be processed, immobilized and ultimately disposed of in geological repositories. In a recent discussion of HLW remediation in the United States, while taking into account the international perspective, Sowder *et al.* (2013) note that “All countries committed to permanent disposal solutions for used fuel and HLW have chosen deep geologic disposal as the principal option.”

The concept and use of borosilicate glass as a primary means to secure HLW is well established, due primarily to the simplicity of the vitrification process, supported by an active industry in glass production. However, some scientists have questioned the use of glass from the perspective of aqueous durability, especially at elevated temperature, and the potential for higher dissolution rates in geological repositories, resulting in the release of radionuclides into the environment (e.g. McCarthy, 1977; Ringwood, 1978). Focussed research activities on alternative materials to borosilicate glass began to appear ~40 years ago and have continued to evolve over time. Many of the candidate HLW materials for nuclear waste disposal are designed, at least in part, with knowledge gained from Th-U mineral phases with minimal radiation induced property changes, low dissolution rates and the ability to retain radionuclides for geological time periods in aqueous fluids. During the 1970s, ceramic nuclear waste forms such as Supercalcine and the Synroc suite of materials appeared and these were based on mutually compatible mineral phases in simplified systems such as $\text{Al}_2\text{O}_3\text{-SiO}_2\text{-P}_2\text{O}_5\text{-CaO-ZrO}_2$ and $\text{Al}_2\text{O}_3\text{-CaO-TiO}_2\text{-ZrO}_2\text{-BaO}$, respectively (McCarthy, 1976; Ringwood *et al.*,

1979, 1981). Indeed, a group of materials referred to as ‘tailored ceramics’ appeared during this time based on high silicate-phosphate, Al, or Ti bulk compositions, for which natural analogues were understood to play a role in the assessment of the phase stability under repository conditions (Clarke *et al.*, 1982; Harker, 1988).

This present paper is not intended to be an exhaustive review of nuclear waste form development and performance testing. Instead, a brief summary is presented of the role that minerals have played in these areas, mainly from the perspective of our own research activities. Furthermore, the focus is on materials and therefore minerals that are specifically related to wastes generated by reprocessing of commercial spent fuel and various legacy materials containing actinide elements. This excludes the area of direct disposal of spent fuel, so the behaviour of ThO_2 and UO_2 in natural systems or their ore deposits will not be discussed here. To gain a perspective on the state of play ~20 years ago, readers interested in spent fuel and natural analogues thereof are referred to the collection of articles published in the *Journal of Nuclear Materials*, **190**, 1–348 and the December 1994 issue of the *MRS Bulletin*, **XIX** (e.g. Forsyth and Werme, 1992; Shoesmith and Sunder, 1992; Janeszc and Ewing, 1992; Isobe *et al.*, 1992; Johnson and Werme, 1994). These special issues also contain several interesting articles on nuclear waste glasses (e.g. Bates *et al.*, 1992; Oversby and Phinney, 1992; Trotignon *et al.*, 1992; Grambow, 1994) and other aspects of nuclear waste disposal. This present paper concentrates on the most common natural analogues that have been proposed as waste-form phases and also studied in the laboratory: pyrochlore, zirconolite, brannerite, crichtonite (mainly davidite), zircon (with comments on thorite) and monazite. A broader description of nuclear waste forms, natural analogues and more detailed discussions of laboratory data including radiation damage effects can be found elsewhere (Weber *et al.*, 1998, 2009; Lumpkin, 1999, 2001, 2006; Stefanovsky *et al.*, 2004; Lumpkin *et al.*, 2004; Lumpkin and Geisler-Wierwille, 2012; Vance, 2012).

Chemical and isotopic composition of nuclear wastes

Nuclear materials arising from reprocessing of HLW are exceedingly complex, containing more

than half of the elements from the periodic table and even larger numbers of radionuclides due to the presence of fission products and daughter products *via* radioactive decay (Stefanovsky *et al.*, 2004). These elements and radionuclides can generally be classified as follows: (1) fission products: Sr, Y, Mo, Tc, Ru, Rh, Pd, Ag, Te, I, Cs, La, Ce, Pr, Nd, Pm, Sm, Gd and Eu, among others; (2) corrosion products: Al, Si, Fe, Zr, Mo and their activation products such as ^{51}Cr , ^{54}Mn , ^{59}Fe , ^{58}Co , ^{60}Co , ^{122}Sb and ^{124}Sb ; (3) fuel components and transmutation products: U, Np, Pu, Am and Cm; and (4) processing contaminants: including F, Na, Mg, S, Cl, K, Ca and Fe.

Many of the isotopes of these elements are long-lived (e.g. ^{99}Tc , ^{129}I , ^{135}Cs , ^{239}Pu) and require careful consideration for storage in geological repositories, whereas others are short-lived (e.g. ^{90}Sr , ^{137}Cs) and have the potential to be separated out of the waste stream for surface storage in special-purpose waste forms or other appropriate containment systems.

Waste forms drive natural analogue studies

A summary of the various types of ceramic nuclear waste forms that have been developed, to various levels, either as alternatives to borosili-

cate glass for HLW or as special-purpose materials for separated HLW or legacy wastes is given in Table 1. These materials have been designed with a number of criteria in mind (see Stefanovsky *et al.*, 2004): (1) high durability in aqueous fluids; (2) resistance to changes in properties due to radiation damage; (3) thermodynamic stability over long periods of time; (4) high-waste loadings and hence minimum volume for the waste form; (5) suitable properties such as hardness, elastic modulus and thermal conductivity; (6) safe, reliable and cost effective production processes; and (7) compatibility with geological environments.

Note points (1), (3) and (7) which relate to the ability of the waste form to resist dissolution and to retain various radionuclides for up to a million years in some scenarios. Ultimately, high aqueous durability in many materials will relate to the kinetics and mechanisms of geochemical alteration at low temperatures, as many waste form phases are not generally chosen to match specific geological host rocks in repositories and therefore may not be thermodynamically stable with respect to a given rock–water system.

Crystalline ceramic nuclear waste forms have been designed as polyphase materials for the disposal of HLW from power plants (see

TABLE 1. Summary of waste forms for HLW from reprocessing of commercial spent fuel and special purpose formulations for Pu and actinides.

Waste Form	Main phases	Application/waste loading
Supercalcine	Apatite, corundum, fluorite, monazite, pollucite, spinel	HLW from reprocessing, up to 70 wt.%
Synroc - C	Zirconolite, perovskite, hollandite, rutile	HLW from reprocessing, up to 20 wt.%
Synroc - D	Zirconolite, perovskite, spinel, nepheline	US defense wastes, 60–70 wt.%
Synroc - F	Pyrochlore, perovskite, uraninite	Conversion of spent fuel, ~50 wt.%
Tailored ceramics	Magnetoplumbite, zirconolite, spinel, uraninite, nepheline	US defense wastes to 60 wt.% or greater
Pyrochlore	Pyrochlore, zirconolite-4M, brannerite, rutile	Separated actinides or Pu up to ~35 wt.%
Zirconolite	Zirconolite, rutile	Separated actinides up to ~25 wt.%
Monazite	Monazite	Actinide-lanthanide wastes (up to ~25 wt.% actinides)
Zircon	Zircon	Pu-rich legacy wastes (10 wt.% Pu)
Cubic zirconia	Single-phase fluorite type solid solution or two phases (Zr and Th rich)	Pu-rich legacy wastes (~10 wt.% Pu)
Glass-ceramics	Titanite, zirconolite, pyrochlore, perovskite, nepheline, sodalite, alumino-silicate glass	Canadian wastes (low actinide content), complex legacy wastes, intermediate level wastes
Others	Kosnarite, murataite, crichtonite, aeschynite–euxenite type AB_2O_6 structure types	Proposed as host phases for actinides and various fission products

Ringwood *et al.*, 1988 and references therein), or as specialist materials for the encapsulation of actinides and fission products that would arise from the possible separation of HLW into various fractions, or for Pu from dismantled nuclear weapons or other industrial processes. Although some waste forms are conceived as single-phase ceramics such as the pyrochlore-based materials designed in ~1997 for the US Plutonium Immobilization Project (e.g. Ewing *et al.*, 2004), the actual waste form may contain additional phases in the final product in order to meet a combination of practical requirements, including processing methods, incorporation of impurities and, criticality, control (Strachan *et al.*, 2005; Icenhower *et al.*, 2006).

As noted in the Introduction, ceramic materials like Supercalcine and Synroc represent the first generation of nuclear waste forms based on Th-U minerals and have the added capability of incorporating a wide range of fission products and other elements. Typical crystalline phases in Supercalcine formulations are silicate apatite, spinel, corundum, fluorite-type oxides, pollucite and monazite. In Synroc-C, for example, zirconolite is designed to be the primary host phase for actinides, perovskite is the host phase for Sr and hollandite is the host phase for Cs. Synroc in its various forms is perhaps the most studied ceramic waste form to date, with numerous reports and publications on the processing conditions, crystal chemistry, element partitioning, aqueous durability and radiation damage effects (Ringwood *et al.*, 1988; Smith *et al.*, 1992; Vance, 1994; Lumpkin *et al.*, 1995; Lumpkin, 2001, 2006; Begg, 2003).

Repositories define the conditions

Strategies for the location of ceramic nuclear waste form packages and associated engineering barriers in geological repositories are focussed largely on clay formations or crystalline rocks, including the option for disposal in near-surface vaults or in deep bore holes. A major project for the development of a repository in clay is underway in Belgium, and a Canadian concept for a repository in a clay-limestone formation has been proposed. In Finland and Sweden, research facilities have been established in granitic rocks, although these would ultimately house spent fuel, and another underground research facility has been in operation for some time in Switzerland. In the US, existing facilities at Yucca Mountain,

Nevada and the Waste Isolation Pilot Plant in southern New Mexico are developed in volcanic rock and within a salt formation, respectively. In general, the near-surface repositories will experience temperatures of ~25°C depending on the local climate. Conditions in deep bore holes will depend upon the local geothermal gradient and will be in the order of 45–65°C at a depth of 1 km or 125–225°C at a depth of 5 km for temperature gradients of 20–40°C km⁻¹. Depending on a number of factors, including source and flow rate, ground-water compositions in the different types of repositories will reflect various degrees of equilibration with clay and carbonate minerals and silica-saturated granitic/volcanic rock systems. In many potential repository systems in crystalline rocks, the groundwater is stratified and changes in composition, source and age with increasing depth from Na–Cl–HCO₃ to Na–Cl–SO₄ to Na–Cl to Ca–Na–Cl brines, reflect the influence of different water sources and ages (King *et al.*, 2002). A similar situation is encountered at the Bruce site in Ontario, Canada, where the geological strata consist of shale and limestone formations (Jensen *et al.*, 2009).

Natural analogue host rocks and thermal history

Natural samples of the Th-U minerals of interest as analogues for nuclear waste forms occur generally either in concentrated form in ore deposits or as accessory minerals in rocks with various levels of enrichment in Th, U and other elements including Ti, Fe, Sr, Y, Zr, Nb, Sn, Ba, the lanthanides, Hf, Ta and W, among others. Natural analogues from sedimentary, metamorphic and igneous geological environments have been studied by numerous investigators. These are summarized in Table 2, including a brief indication of the Th-U minerals present in each type of deposit. Sedimentary deposits or products of weathering are of considerable interest as they may provide evidence of enhanced chemical durability at low temperatures. Zircon and monazite represent two very important Th-U minerals that commonly survive weathering and transport and may be recycled in younger sedimentary, metamorphic, or igneous rocks.

Geochronology can provide accurate information on the thermal history of certain natural analogue host rocks by taking advantage of methods that have different closure temperatures. In general, the U-Pb isotopic system returns ages

ROLE OF Th-U MINERALS IN ASSESSING NUCLEAR WASTE FORMS

TABLE 2. Types of geological deposits, mineralogy and selected examples.

Type of deposit	Th-U mineralogy	Examples
Granites (K-rich)	Apatite-zircon-thorite-titanite-allanite	Vosges massif, France
Granites (leucocratic)	Monazite-zircon-apatite-xenotime	Vosges massif, France
Felsic volcanic rocks	Pyrochlore, thorite	Italy
Carbonatite complexes	Nb-rich pyrochlore, perovskite, zirconolite, baddeleyite	Kaiserstuhl, Germany Jacupiranga, Brazil Oka, Quebec, Canada
Nepheline syenites	Pyrochlore, perovskite, zirconolite	Larvik, Norway Lovozero, Russia
Kimberlites	Perovskite	Somerset Island, Canada Matsoku, Lesotho
Hydrothermal veins	Pyrochlore, zirconolite	Adamello, Italy
Contact metamorphic rocks	Zirconolite, perovskite, titanite	Bergell, Switzerland
LCT (Li,Cs,Ta) granitic pegmatites	Zircon-hafnon, thorite, Ta-rich pyrochlore	Harding, New Mexico Tanco, Canada Wodgina, Australia
NYF (Nb,Y,F) granitic pegmatites	Aeschnyite, euxenite, U-Nb-rich pyrochlore, monazite, xenotime, zircon, thorite, brannerite	Madagascar Llano Co., Texas Spruce Pine, North Carolina Ytterby, Sweden
Laterites	Nb-rich pyrochlore	Araxá, Brazil
Placer deposits	Zircon, monazite, brannerite	Stanley, Idaho Sri Lanka
Lunar rocks	Zirconolite, zircon, baddeleyite	Apollo 11,12, 14–17 and Luna 20 landing sites
Chondritic meteorites	Perovskite	Allende

representative of the host rock crystallization, the K-Ar isotopic system and other methods date the post-magmatic phase of cooling, and fission-track dating constrains the final phase of cooling. A pertinent example is that of the Bergell intrusion, in the Swiss-Italian Alps. Geochronological data demonstrate that the eastern part of the Bergell intrusion, where zirconolite is found in the contact aureole, cooled rapidly from $\sim 700^{\circ}\text{C}$ to 300°C in the first 3–4 M.y., then cooled much more slowly to 100°C in the next 15 M.y. (see fig. 5 in Hansmann, 1996). Lumpkin *et al.* (1998) discussed the thermal histories of natural analogue-bearing host rocks in some detail. One advantage of working with late orogenic igneous rocks is that a simple mathematical approach, within the boundaries of reasonable assumptions, can be applied in order to derive the cooling history. With knowledge of the size and emplacement depth of the host rock intrusion, the time scale (t) necessary for thermal decay by conductive cooling can be estimated from the equation:

$$t = h^2/\kappa \quad (1)$$

where h is the intrusion half-width and κ is the thermal diffusivity of the intrusive and country rocks. Calculations with $\kappa = 32 \text{ km}^2 \text{ M.y.}^{-1}$ indicate that carbonatite intrusions, for example, generally cool to the temperature of the regional terrain within 1 M.y. of emplacement. For geothermal gradients of $20\text{--}40^{\circ}\text{C km}^{-1}$, the surrounding rocks would have been at temperatures of $100\text{--}250^{\circ}\text{C}$. Using this approach, Lumpkin *et al.* (1998) estimated that suites of zirconolite samples from different localities would have experienced average temperatures as high as 235°C for the larger igneous intrusions (e.g. Adamello, Italy) to a minimum of $\sim 50^{\circ}\text{C}$ for some carbonatites. For the unusual case in which the carbonatite host rocks have been metamorphosed, such as the pyrochlore-bearing rocks at Blue River, British Columbia, Canada, the thermal history may be dramatically different as shown in Fig. 1. In this case, the regional metamorphism led to an increase in the critical dose for amorphization of pyrochlore due to annealing of alpha-recoil collision cascades. In a recent study of brannerite, Lumpkin *et al.* (2012)

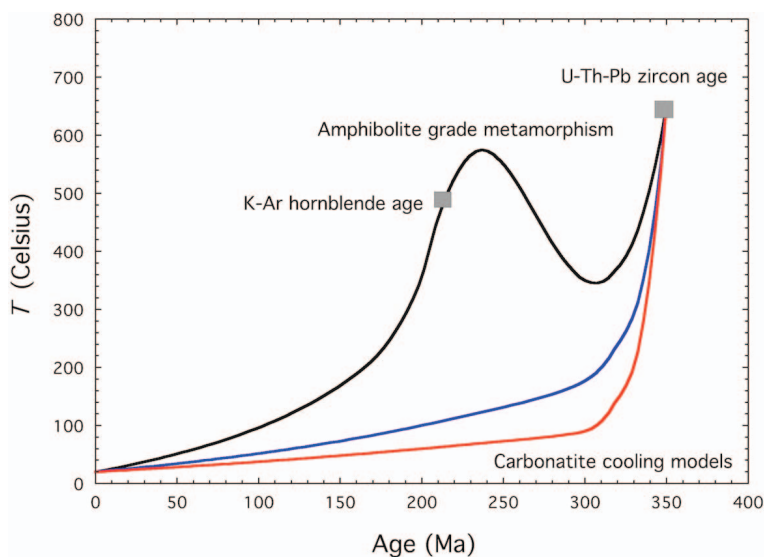


FIG. 1. An illustration of the complex thermal history of metamorphosed pyrochlore-bearing host rocks from Blue River, British Columbia, Canada. The approximate cooling curve is derived from the U-Th-Pb age of zircon together with the K-Ar age of hornblende, the latter age following the peak of amphibolite grade metamorphism that occurred at $t \sim 250$ Ma. Also shown are cooling models (dashed lines) for the original carbonatite intrusion with estimated parameters for the size and depth of emplacement used to construct the curves (see text). The upper and lower dashed lines correspond to models based on geothermal gradients of $40^{\circ}\text{C km}^{-1}$ and $20^{\circ}\text{C km}^{-1}$, respectively.

reconstructed the approximate thermal history experienced by granitic host rocks in the eastern region of South Australia (see fig. 9 in Lumpkin *et al.*, 2012). In this case, the regional metamorphism ($\sim 650^{\circ}\text{C}$ peak at 500 Ma) occurred much later than the crystallization age (~ 1580 Ma), suggesting that the brannerite may have become amorphous, recrystallized and become amorphous again following metamorphism.

Crystal chemistry

Pyrochlore is a derivative of the fluorite structure and corresponds to the general formula $A_2B_2X_6Y$ in which A and B represent 8- and 6-coordinated cation sites and X and Y are 4-coordinated anion sites. In natural samples, A = Na, Ca, Y, lanthanides, actinides and B = Ti, Zr, Nb, Hf, Ta, Sn and W. Many more elements are found in natural samples and hundreds of different stoichiometric and defect pyrochlore compositions have been synthesized (Subramanian *et al.*, 1983; Chakoumakos, 1984). The compositions of most stoichiometric natural pyrochlores can be described in the greatly simplified system

$\text{NaCaNb}_2\text{O}_6\text{F}-\text{NaCaNb}_2\text{O}_6\text{OH}-\text{NaCaTa}_2\text{O}_6\text{F}-\text{NaCaTa}_2\text{O}_6\text{OH}-\text{Ca}_2\text{Nb}_2\text{O}_7-\text{Ca}_2\text{Ta}_2\text{O}_7-\text{CaUTi}_2\text{O}_7-\text{Ln}_2\text{Ti}_2\text{O}_7-\text{Ca}_2\text{TiWO}_7$; however, there are also many other substitution mechanisms possible, including A cation and Y anion vacancies. Prototype waste-form pyrochlores are usually based upon the CaUTi_2O_7 , $\text{Ln}_2\text{Ti}_2\text{O}_7$ and $\text{Ln}_2\text{Zr}_2\text{O}_7$ endmembers and these are actually relatively rare in nature due to factors such as host-rock geochemistry and the formation of other minerals such as UO_2 , TiO_2 , ZrO_2 and ZrSiO_4 in stable phase assemblages.

Zirconolite is a derivative of the fluorite structure type and can be considered as a condensed version of pyrochlore. The prototypical endmember composition is $\text{CaZrTi}_2\text{O}_7$ for the *2M* polytype. Different polytypes (e.g. *3T*, *3O*, *4M*) arise through solid-solution towards lanthanide and actinide endmembers. For example, Vance *et al.* (2002) demonstrated that the substitution of U for Zr in $\text{CaZrTi}_2\text{O}_7$ leads to the phase evolution zirconolite-*2M*, zirconolite-*2M* + *-4M*, zirconolite-*4M*, zirconolite-*4M* + pyrochlore and pyrochlore (CaUTi_2O_7). Actinide (*Act*) and lanthanide (*Ln*) elements may substitute for Ca and Zr with appropriate

charge-balancing mechanisms. Charge compensation may be achieved in some cases *via* substitution of elements like Mg, Al, Fe, Nb, Ta and W for Ti. The observed natural compositions are complex, illustrating a high level of chemical flexibility and this has been confirmed to a large extent through experimental work. Most natural samples can be described by the simplified system $\text{CaZrTi}_2\text{O}_7$ – LnZrTiAlO_7 – CaZrFeNbO_7 – $\text{Ln}_2\text{Ti}_2\text{O}_7$ – ActZrTiFeO_7 . Gieré *et al.* (1998) provided a comprehensive summary of the occurrence and chemical composition of natural zirconolite, wherein they describe 14 possible substitution mechanisms observed in synthetic zirconolite systems and show that all but two of these are also found in natural samples. The range of known compositions of zirconolite samples from carbonatites and metamorphosed carbonate rocks is shown in Fig. 2. Furthermore, in a detailed compilation of analytical data and geological localities, Williams and Gieré (1996) show that zirconolite can contain up to 22.3 wt.% ThO_2 and 24.0 wt.% UO_2 . In general, the compositions of natural zirconolite samples provide broad correspondence with synthetic zirconolites and also with those in nuclear waste forms, therefore the degree of analogy is high from a crystal-chemical perspective.

Brannerite is a monoclinic ($C2/m$) AB_2O_6 oxide consisting of layers of Ti octahedra connected by columns of U octahedra with structural similarities to the TiO_2 polymorphs. In the pure form (UTi_2O_6) it contains ~62 wt.% UO_2 and is a minor phase in some of the pyrochlore-based compositions designed for the disposal of Pu. Nevertheless, brannerite may account for a significant fraction of the total U and Pu inventory in these waste forms (Thomas and Zhang, 2003). Natural brannerite in a relatively unaltered form can incorporate up to 7 wt.% CaO, 5 wt.% Y_2O_3 , 3 wt.% Ln_2O_3 and 15 wt.% ThO_2 substituting primarily for U. Incorporation of lower valence A cations may be charge balanced in part by oxidation of some U^{4+} to U^{5+} and/or U^{6+} ions. Natural samples may also incorporate minor quantities of Al, Fe and Nb, substituting primarily for Ti. Furthermore, minor amounts of radiogenic Pb may be present and some Si has also been reported (Lumpkin *et al.*, 2012), although the role of Si in the structure of crystalline brannerite is unknown.

The crichtonite structure type, a rhombohedral family of layered compounds based on the ideal

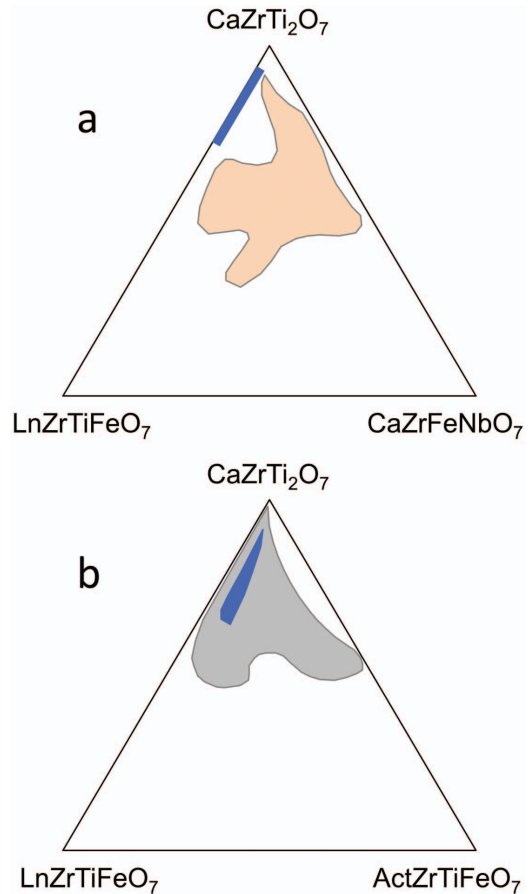


FIG. 2. Ternary diagrams showing the approximate ranges of compositions of natural zirconolite samples from (a) carbonatites and (b) metamorphosed carbonate rocks. Approximate ranges of zirconolite compositions (blue line and field, wherein the small trivalent cation is Al instead of Fe) from various polyphase Synroc formulations are included for reference. Adapted from Gieré *et al.* (1998).

formula $\text{AM}_{21}\text{O}_{38}$, was proposed as a possible host phase for actinides and fission products in nuclear waste forms (Gong *et al.*, 1995). Crichtonite group minerals can contain a wide range of cations, with A = Pb, Ba, Sr, Ca, K, Na and light lanthanides and M = Mg, Al, Ti, V, Cr, Mn, Fe, Zn, Zr, Th, U, Y and heavy lanthanides, among others. Loveringite, approximately $(\text{Ca,Sr,Na})(\text{Ti,Al,Fe,Zr})_{21}\text{O}_{38}$, is a common accessory phase in certain Synroc formulations containing Fe, where it typically contains ~1–2 wt.% Ln_2O_3 and up to 0.5 wt.% UO_2 (Lumpkin *et al.*, 1995). Apart from the large Al

content (which proxies for Fe and Cr), the compositions of the synthetic Synroc research samples are very similar to those of natural loveringites from the Jimberlana layered ultramafic igneous intrusion in Western Australia (Campbell and Kelly, 1978; Gatehouse *et al.*, 1978). Other crichtonite-group minerals such as crichtonite *sensu stricto* with A = Sr (Grey *et al.*, 1976), dessauite with A = Sr, Pb (Orlandi *et al.*, 1997), landauite with A = Na (Grey and Gatehouse, 1978) and davidite with A = Ln, Th, U, Y, Sr, Pb (Gatehouse *et al.*, 1979; Lumpkin *et al.*, 2013) suggest that there is considerable potential for this structure type as a host phase for smaller amounts of actinides and fission products together with processing contaminants and corrosion products in nuclear waste form materials.

Perovskite is an ABX_3 structure type wherein the major A cations include Na, Ca, Sr and light lanthanides (La–Nd). The major B cations are predominantly Ti, Fe and Nb with minor Zr in certain occurrences. Most perovskite compositions can be represented in the system $CaTiO_3$ – $NaNbO_3$ – $Na_{0.5}Ln_{0.5}TiO_3$ – $CaFe_{0.5}Nb_{0.5}O_3$ – $SrTiO_3$ (Mitchell, 2002). Composition ranges are summarized in Fig. 3 by way of three ternary diagrams. The non-stoichiometric composition $CaNbO_{3.5}$ (or $Ca_2Nb_2O_7$) is also thought to be a significant component in certain natural samples, but this would not be the case in nuclear waste forms due to very low Nb contents in most waste materials. The Zr and Th contents are typically below 0.3 wt.% ZrO_2 and 4.5 wt.% ThO_2 in most occurrences; however, up to ~3.5 wt.% Zr has been reported in samples from kimberlites and a few high-Th perovskites have been described with up to ~18.5 wt.% ThO_2 (Mitchell and Chakmourandian, 1998) and these are important for the assessment of radiation damage. From a chemical viewpoint, natural perovskites are good analogues for examining the behaviour of certain

fission products, especially Sr and the light lanthanide elements, together with Na (e.g. Japanese waste stream) and other processing contaminants or corrosion products. The relatively low levels of Th and U are confirmed by detailed studies of element partitioning, e.g.

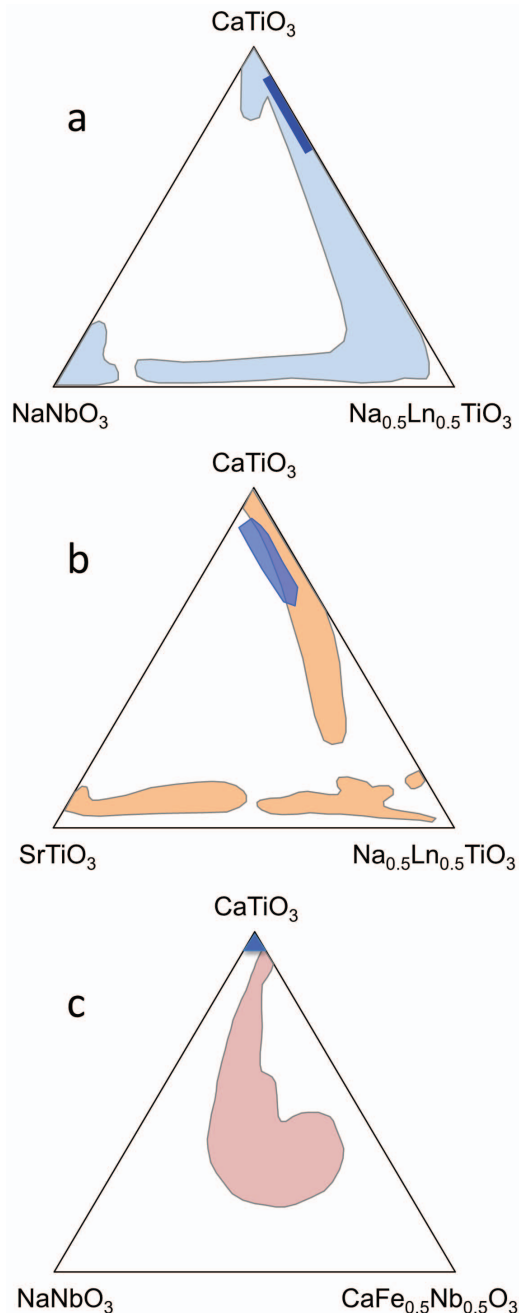


FIG. 3. Ternary diagrams showing the approximate ranges of compositions of natural perovskite samples from (a) kimberlites, alkaline ultramafic rocks, carbonatites, (b) K- and Na-rich syenites, fenites, lamproites, orangeites and (c) Oka, Kaiserstuhl and Magnet Cove carbonatite complexes with Fe-Nb-rich perovskites. Approximate ranges of perovskite compositions (blue line, field and small triangle) from various polyphase Synroc formulations are included for reference. Adapted from Mitchell (2002).

between zirconolite and perovskite, in various Synroc formulations (Lumpkin *et al.*, 1995).

Zircon, an ABO_4 structure type that generally conforms closely to the composition $ZrSiO_4$, is a common accessory mineral found in a variety of geological environments and is perhaps the quintessential mineral for geological age dating. The major elemental impurity in natural zircon is Hf, which substitutes for Zr. The Hf content is generally $\sim 1\text{--}2$ wt.% HfO_2 ; however, in LCT-type granitic pegmatites this may be much larger, with extensive solid-solution to near endmember hafnion, $HfSiO_4$. Trace to minor amounts (generally 5000 ppm or less) of other elements may be present, including Ca, lanthanides and actinides on the Zr site and P on the Si site. Higher concentrations have been reported, but are exceptional. Although natural zircon has been studied extensively, the degree of analogy with waste forms designed for Pu with loadings of ~ 10 wt.% (e.g. Ewing *et al.*, 1995) is somewhat limited by the low actinide contents. Other minerals with the zircon structure, e.g. thorite ($ThSiO_4$) and coffinite ($USiO_4$) represent the extreme levels of actinide incorporation. These minerals contain ~ 81.5 wt.% ThO_2 and ~ 81.8 wt.% UO_2 in pure form, respectively, but may be lower in the event of extensive chemical substitution in geological systems. In the Harding granitic pegmatite, for example, thorite may exhibit extensive solid-solution in the system $ThSiO_4\text{--}Ca_{0.5}Th_{0.5}PO_4\text{--}Ca_{0.5}Th_{0.5}VO_4\text{--}YPO_4\text{--}YVO_4\text{--}BiVO_4$ (Lumpkin and Chakoumakos, 1988), presenting some interesting options for the design of actinide waste forms with higher waste loadings and improved radiation tolerance.

Monazite also has ABO_4 stoichiometry, but the crystal structure is monoclinic and consists of chains of alternating BO_4 tetrahedra and AO_9 polyhedra. These chains are cross linked by edge sharing with the AO_9 polyhedra, effectively closing off open tunnels and creating a structure that is $\sim 10\%$ denser than the zircon structure type. Ideally, having the composition $LnPO_4$, with $Ln = La, Ce, Pr$ and Nd together with smaller amounts of $Sm\text{--}Lu$ and Y , natural monazite exhibits extensive solid-solution towards other endmembers with $A = Ca, Th$ and U . Most natural samples are thus defined in the system $LnPO_4\text{--}Ca_{0.5}Th_{0.5}PO_4\text{--}ThSiO_4\text{--}USiO_4$ and may contain up to 16 wt.% UO_2 and 52 wt.% ThO_2 (Boatner and Sales, 1988; Förster, 1998; Boatner, 2002). In a detailed study of monazite in the peraluminous granites of the Erzgebirge–Fichtelgebirge region

of Germany, including a summary of monazite from other localities, Förster (1998) has shown that there is effectively a complete range of compositions along the joins $LnPO_4\text{--}ThSiO_4$ and $LnPO_4\text{--}Ca_{0.5}Th_{0.5}PO_4$ (Fig. 4). Furthermore, monazite from alkaline rocks may contain up to ~ 9 wt.% SrO, indicating solid-solution towards an endmember of the form $Sr_{0.5}Th_{0.5}PO_4$ (Chakhmouradian and Mitchell, 1998). More recently, Pršek *et al.* (2010) have reported metamorphic-hydrothermal monazites that contain up to ~ 11.1 wt.% SO_3 , 5.0 wt.% CaO and 8.7 wt.% SrO, consistent with a general chemical substitution of the form $A^{2+} + B^{6+} \leftrightarrow A^{3+} + B^{5+}$ in this particular case.

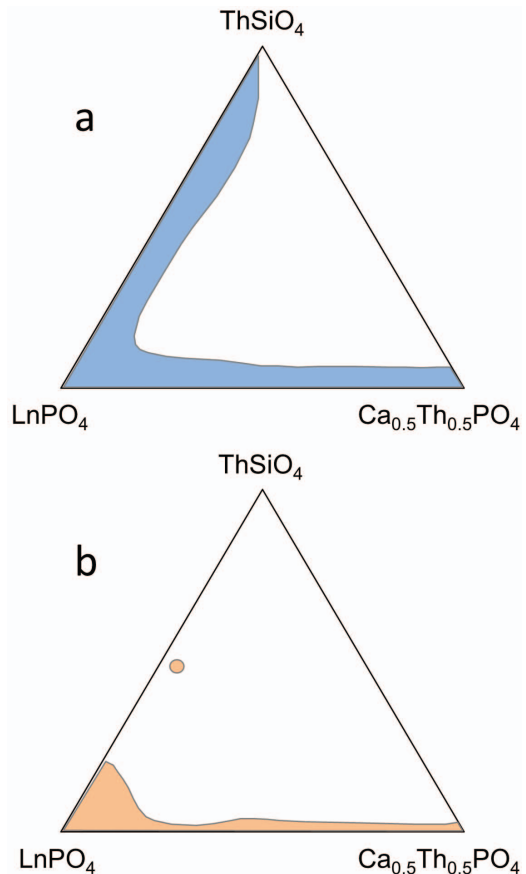


FIG. 4. Ternary diagrams depicting the composition ranges of monazite from (a) various granites, pegmatites, migmatites and granulite and (b) the peraluminous granitic rocks of the Erzgebirge–Fichtelgebirge region, Germany. Adapted from Förster (1998).

Geochemical behaviour

The petrography, chemistry and geochemical alteration of natural pyrochlore-group minerals have been studied in some detail, showing that natural samples in the system $\text{NaCa}(\text{Nb}, \text{Ta})_2\text{O}_6(\text{F}, \text{OH})-\text{Ca}(\text{Th}, \text{U})\text{Ti}_2\text{O}_7-\text{Ln}_2\text{Ti}_2\text{O}_7$ are susceptible to alteration *via* reaction with aqueous fluids over a range of conditions involving pressure, temperature and fluid composition. In hydrothermal systems where conditions approximate to $\sim 200-350^\circ\text{C}$ and low hydrostatic pressure, the principal result of alteration is the loss of Na and F and this may be combined with cation exchange for Sr, Ba, REE and Fe. Further removal of Na, F, Ca and O may occur in low-temperature hydrothermal or weathering environments, especially in laterites where large volumes of water may pass through the local system, resulting in *A*-site, *Y*-site and *X*-site vacancies, coupled with the uptake of K, Sr, Cs, Ba, Ce and Pb together with H_2O and H^+ (Nasraoui *et al.*, 1999; Lumpkin and Mariano, 1996; Lumpkin and Ewing, 1992, 1995, 1996; Wall *et al.*, 1996; Williams *et al.*, 1997; Chakhmouradian and Mitchell 1998; Wise and Černý, 1990; Ohnenstetter and Piantone, 1992; Wall *et al.*, 1999; Gieré *et al.*, 2001). The most appropriate

pyrochlore natural analogues from a chemical viewpoint are the Ti-rich examples from hydrothermal veins in the contact metamorphic zone adjacent to the Adamello igneous massif in northern Italy. These pyrochlores contain 29–34 wt.% UO_2 and can be described in the system $\text{CaUTi}_2\text{O}_7-\text{Ca}_2\text{TiWO}_7-\text{Ca}_2\text{Nb}_2\text{O}_7-\text{Ln}_2\text{Ti}_2\text{O}_7$ with $\text{Ti}/(\text{Nb}+\text{Ta})$ ratios of $\sim 10-15$, so they are among the most Ti-rich natural pyrochlores known. Apart from minor hydration of the rims of individual crystals, these samples demonstrate quantitative retention of U and Th for time periods of 40 M.y., even though the crystals experienced cumulative total alpha-decay doses of $3-4 \times 10^{16}$ α/mg (Lumpkin *et al.*, 1999). Other pyrochlores, having intermediate *B*-site compositions with $\text{Ti}/(\text{Nb}+\text{Ta})$ ratios of $\sim 0.6-1.8$, have been described from several localities (e.g. Lumpkin and Ewing, 1996; De Vito *et al.* 2006). Alteration effects in these samples range from simple hydration coupled with minor changes in composition to more extensive removal of *A*-site cations. Figure 5 shows that in most cases, the Th and U contents remain nearly constant in altered pyrochlores with Ta, Nb and Nb-Ti as the dominant *B*-site cations. In examples from the NYF granitic pegmatites of Madagascar, when the Ca content falls below 0.2–0.3 atoms

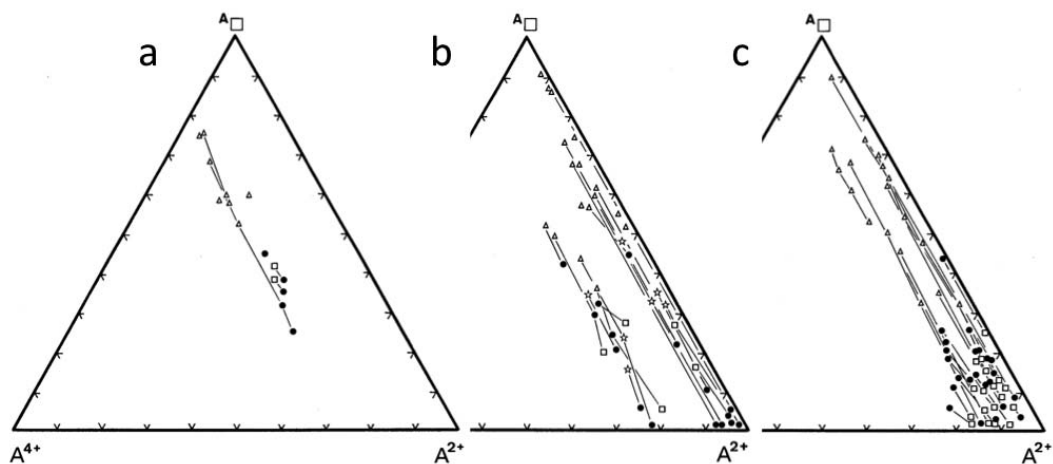


FIG. 5. Ternary diagrams showing the alteration of pyrochlore-group minerals from granitic pegmatites, nepheline syenites and carbonatites. Figures depict variations in *A* cations and vacancies, with $\text{A}^{2+} = \text{Ca}, \text{Mn}, \text{Fe}, \text{Sr}$; $\text{A}^{4+} = \text{Th}, \text{U}$; and A^{\square} = vacancies (disregarding possible occupancy by H_2O). (a) Samples mainly from NYF granitic pegmatites and carbonatites, $\text{B} = \text{Nb}$ and Ti with $\text{Ti}/(\text{Ti}+\text{Nb}) \approx 0.8-1.2$. (b) Samples primarily from NYF granitic pegmatites with $\text{B} = \text{Nb}, \text{Ta}$ and Ti with $\text{Ti}/(\text{Ti}+\text{Nb}+\text{Ta}) \leq 1.0$ and $\text{Nb} > \text{Ta}$. (c) Samples from LCT granitic pegmatites with $\text{B} = \text{Nb}, \text{Ta}$ and Ti with $\text{Nb} < \text{Ta}$ and low Ti contents. Lines show the change in composition upon alteration: filled circles = unaltered and unfilled symbols = altered pyrochlore (squares \sim high temperature, stars \sim intermediate temperature and triangles \sim low temperature alteration). From Lumpkin (1989).

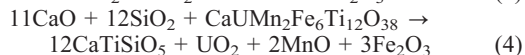
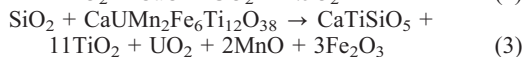
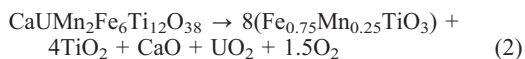
per formula unit, these pyrochlores show evidence for partial recrystallization to a new phase assemblage consisting of liandratite (ideally UNb_2O_8) + rutile (or anatase). The bulk U content appears to be maintained in most samples; however, Lumpkin and Ewing (1996) described one sample from Madagascar wherein ~20% of the U present at the time of alteration was removed from the altered pyrochlore, but redeposited in the adjacent host rock as liandratite.

Rasmussen and Fletcher (2004) proposed that zirconolite may become the principal mineral for age determination in mafic igneous rocks due to its ability to retain radiogenic Pb. Their analysis of 1200 Ma dolerite intrusive rocks from Western Australia demonstrated that zirconolite returned the same $^{207}\text{Pb}/^{206}\text{Pb}$ age as zircon and baddeleyite, but the zirconolite age was much more precise (by factors of ~3.3 and 13, respectively). This appears to confirm the earlier isotopic age dating work by Oversby and Ringwood (1981) and the electron microscopy studies by Ewing *et al.* (1982), which demonstrated that natural zirconolite exhibits closed-system behaviour for U, Th and Pb for up to 650 M.y. with little, if any, evidence of geochemical alteration. Nevertheless, zirconolite does show evidence for interaction with hydrothermal fluids, in particular those with SiO_2 as a significant component. Lumpkin *et al.* (1994) and Hart *et al.* (1996) described the alteration of amorphous zirconolite from the 2060 Ma carbonatite complex of Phalaborwa, South Africa in some detail. Electron microprobe analyses, element mapping and backscattered electron images demonstrate that the alteration is localized along cracks and resulted in the incorporation of Si and loss of Ti, Ca and Fe. However, in these samples the Ln, Y, Th and U contents remained relatively constant across the alteration zones. Radiogenic Pb appears to have been mobile and precipitated mainly within the altered areas as galena. In certain carbonatites, electron microanalysis and imaging studies by Bulakh *et al.* (1998) and Williams *et al.* (2001) reveal that zirconolite may be replaced along cracks and within μm -sized domains by an unidentified Ba–Ti–Zr–Nb–Act silicate phase, suggesting that zirconolite may not be stable in the presence of relatively low-temperature hydrothermal fluids enriched in aqueous silicate species.

Lumpkin *et al.* (2012) presented an evaluation of geochemical alteration effects in a small suite

of natural brannerites ranging in age from ~10 to 1580 Ma. Some of the samples appear to be unaltered, whereas others exhibit only minor alteration, located usually within veinlets or around the rim of the sample. The remaining samples are altered extensively and may contain secondary phases such as TiO_2 polymorphs, galena and thorite. This group of samples also tend to have the greatest geological ages. Geochemical alteration of brannerite resulted in the incorporation of up to 17 wt.% SiO_2 coupled with the loss of up to 90 wt.% of U present at the time of alteration event. Radiogenic Pb tends to migrate out of unaltered brannerite due to lack of suitable sites. However, in some cases Pb is retained in the altered brannerite at levels above the nominal concentration expected from radiogenic decay. This may be due to the fact that the structure of altered brannerite approximates to a Ti–Si–O glass-like network wherein radiogenic Pb is more comfortable as a network modifier. The aqueous dissolution of synthetic brannerite, pyrochlore and zirconolite has been studied to a certain extent in the laboratory, typically at temperatures of 25–90°C, pH = 2–12 and in pure water (Roberts *et al.*, 2000; Zhang *et al.*, 2001, 2003). Although all three phases exhibit a weak minimum in the release of U near pH = 8, the relative behaviour of the three phases is consistent over the entire pH range with the release of U occurring in the order zirconolite < pyrochlore < brannerite.

Crichtonite-group minerals have not received much attention in the context of nuclear waste form development; however, recent work shows that davidite may be altered to new phase assemblages consisting of either ilmenite + rutile or titanite ± rutile in natural systems (Lumpkin *et al.*, 2013). The following simplified reactions were proposed based on microscopic observations of several samples from Arizona and South Australia:



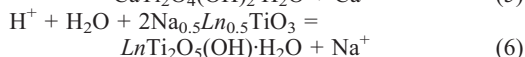
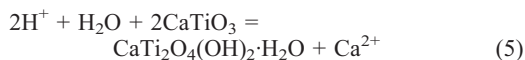
The alteration of davidite to ilmenite + rutile, accompanied by the release of Ca and U and the potential role of oxygen in the local system is represented by equation 2. Equations 3 and 4 illustrate how the chemical potentials of SiO_2 and

CaO may influence the relative amounts of titanite and rutile formed during the breakdown of davidite (see Fig. 6).

In carbonatites from Brazil, Mariano (1989) has documented the low-temperature alteration of perovskite to secondary phases including anatase, cerianite, monazite and crandallite-group minerals during weathering and laterite formation and Banfield and Veblen (1992) proposed that the breakdown of perovskite to anatase (and $\text{TiO}_2\text{-B}$) involves a topotactic

relationship with the framework of TiO_6 octahedra in perovskite. This is consistent generally with laboratory dissolution studies of Synroc-C and synthetic perovskite in pure water at temperatures above 100°C (Smith *et al.*, 1992; Zhang *et al.*, 2005) and other studies of the thermodynamics of perovskite (e.g. Nesbitt *et al.*, 1981).

At higher temperatures in alkaline igneous rocks, Mitchell and Chakmouradian (1998) have described the alteration of perovskite to kassite, anatase, titanite, calcite and ilmenite in the presence of a CO_2 - and SiO_2 -rich fluid phase. Furthermore, Lumpkin *et al.* (1998) and Chakmouradian *et al.* (1999) described the hydrothermal alteration of Na-bearing perovskite (ideally $\text{Na}_{0.5}\text{Ln}_{0.5}\text{TiO}_3$) to lucasite, $\text{LnTi}_2\text{O}_{6-x}(\text{OH},\text{F})_x\cdot\text{H}_2\text{O}$. Reactions proposed for the breakdown of perovskite to kassite or lucasite are given below:



In spite of the above geochemical observations, many perovskite samples are found in a relatively unaltered state in terms of major and minor element chemistry (Mitchell, 2002). Isotopic age dating studies have also demonstrated that perovskite can remain a closed system with regard to the Th-Pb, U-Pb, Sr and Nd contents and isotopic compositions (Oversby and Ringwood, 1981; Mitchell *et al.*, 2011).

Highly crystalline natural zircon with low Th and U content is resistant to aqueous dissolution and chemical alteration over a range of conditions. However, as discussed later in this paper, zircon can be extensively radiation damaged or rendered amorphous with only a few wt.% of Th and U, depending on the geological age. Chakoumakos *et al.* (1987) demonstrated the important relationship between anisotropic volume expansion and cracking in zoned zircon crystals as a function of alpha-decay dose – this is a fundamental aspect of behaviour of zircon in rocks and in nuclear waste forms. In 1000 Ma zoned zircons from Ontario, Canada, the rims of the crystals are fractured extensively and this allowed fluids to penetrate through to the cores that were rendered amorphous due to the presence of only 1–2 wt.% $\text{ThO}_2 + \text{UO}_2$ (Lumpkin, 2001). Altered areas of the cores of these crystals gained up to 4.1 wt.% CaO and small amounts of Al and

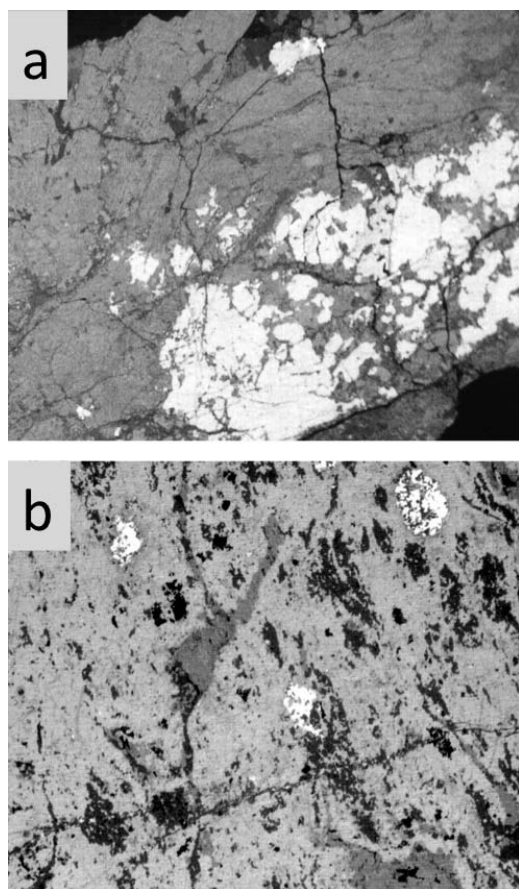
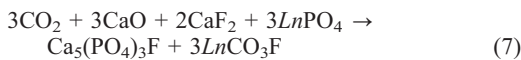


FIG. 6. Backscattered electron images showing alteration of davidite to new phase assemblages. (a) Fully amorphous davidite (white) from Pima County, Arizona, USA replaced by titanite (medium grey) + minor rutile (darker grey). Width of image = 5 mm. (b) Fully amorphous davidite (lighter grey) from Crocker's Well, South Australia, showing alteration to ilmenite (medium grey) + rutile (black), with small inclusions of thorite (white). Width of image = 1 mm.

Fe, but appear to have lost ~40% of the original amount of U. Another example of alteration was described by Geisler *et al.* (2003) for hydrothermal alteration of 619 Ma zoned zircon from a post-tectonic granite, Eastern Desert, Egypt, at temperatures estimated to be 100–200°C. In this case, alteration of the U- and Th-rich zones led to an uptake of Al, Ca, Mn, Fe, light *Ln* elements and H₂O, with loss of Zr, Si and radiogenic Pb. Natural zircons from Sri Lanka have also been used in laboratory dissolution experiments (Geisler *et al.*, 2001). Samples with a range of alpha-decay dose and structural damage levels were subjected to hydrothermal treatment in 2 M CaCl₂ at *T* = 450°C and *P* = 1.3 kbar for 744 h. Under these conditions, the zircon grains developed reaction rims that increased in thickness as a function of the cumulative alpha-decay dose (see fig. 2 in Geisler *et al.*, 2001). The altered rims are recrystallized and exhibit strong enrichment in Ca, H₂O and depletion in Zr, Si and radiogenic Pb. Furthermore, Th was lost from the altered rim of the sample with the largest dose, but not U. Based on the commonly observed alteration of radiation damaged zircons, it is not surprising to find that thorite is altered extensively in natural systems, resulting in hydration, loss of Si, radiogenic Pb and sometimes producing secondary galena in the presence of S-bearing fluids (e.g. Frondel, 1958; Staatz *et al.*, 1976).

Monazite is often regarded as a mineral that is resistant to dissolution and the mineral is common as an ore of light lanthanide elements in beach sands. However, there have been several reports describing alteration of monazite in a range of aqueous fluids. In the Bayan Obo rare-earth deposits, monazite breaks down to apatite and bastnaesite in the presence of Ca- and F-bearing hydrothermal fluids (see fig. 3 in Kynicky *et al.*, 2012). This reaction may be written as follows:



Interactions between monazite and evolving igneous (granitic) and metamorphic fluids at elevated temperature and pressure (above the conditions expected for geological repositories) have provided evidence for monazite breakdown. Ondrejka *et al.* (2012) recently reported on the two-stage breakdown of monazite to apatite and a Th-silicate phase followed by allanite and clinozoisite in orthogneiss from the Western Carpathians, Slovakia and at somewhat lower temperatures of ~400°C. Townsend *et al.* (2000)

described the replacement and recrystallization of monazite and associated chemical effects such as radiogenic Pb loss and minor changes in the amounts of Th, Ca and Si. In two different geological occurrences where hydrothermal alteration occurred at temperatures of ~170–340°C in the presence of a saline aqueous fluid phase, Poitrasson *et al.* (1996, 2000) documented that the chemical exchange reactions $2\text{Ln}^{3+} \rightarrow \text{Ca}^{2+} + \text{Th}^{4+}$ and $\text{Ln}^{3+} + \text{P}^{5+} \rightarrow \text{Th}^{4+} + \text{Si}^{4+}$ took place. Furthermore, in monazite the *Ln* elemental distributions also vary as a result of the different conditions and reaction mechanisms. In a study of monazite from the Steenkampskraal mine, South Africa, Read *et al.* (2002) have shown that the heavy *Ln* and Y are released and precipitated locally as secondary phosphate minerals, U is released to the fluid phase, while the light *Ln* elements are retained in altered monazite. Mathieu *et al.* (2001) studied monazite from Lower Proterozoic sandstones of the Franceville basin, Gabon, reporting the alteration of monazite to a Th-silicate phase in the presence of a diagenetic brine, resulting in loss of light *Ln* elements and U to the fluid phase. Other studies (e.g. Cuney and Mathieu, 2000; Hecht and Cuney, 2000) suggest that Th is less mobile than the lanthanides and Y and is concentrated into Th-bearing alteration products. In granitic pegmatite systems, Hetherington and Harlov (2008) report that that monazite is subjected to a chemical refinement process during interaction with an evolving fluid phase containing Na, K and F, leading to the breakdown of high Ca-Th-U-Si monazite to an assemblage of near endmember *LnPO*₄ monazite + thorite + uraninite *via* a coupled dissolution-reprecipitation mechanism. Laboratory experiments conducted on natural monazite at temperatures of 50–229°C and pH of 1.6 to 10 in Ti-mixed flow reactors (Oelkers and Poitrasson, 2002) yield dissolution rates ~5–8 orders of magnitude lower than those of natural glasses, with a minimum release rate at neutral pH values, an approximately stoichiometric release of light lanthanides and a non-stoichiometric release of Th at low pH due to precipitation of a secondary Th phase.

Radiation damage effects

The total alpha-decay dose *D* can be calculated for any Th-U mineral based upon the decay of ²³⁸U, ²³⁵U and ²³²Th to the stable isotopes ²⁰⁶Pb, ²⁰⁷Pb and ²⁰⁸Pb, respectively:

$$D = 8N_{238}(e^{\lambda_{238}t} - 1) + 7N_{235}(e^{\lambda_{235}t} - 1) + 6N_{232}(e^{\lambda_{232}t} - 1) \quad (8)$$

In equation 8, t is the geological age, N represents the present-day concentration of the parent isotope and λ is the decay constant. In the absence of isotopic determinations of the ^{238}U and ^{235}U contents, an assumed isotopic composition of 99.28% ^{238}U and 0.72% ^{235}U may be used; however, in general, the second term in the

equation can also be ignored without introducing significant errors into the calculated dose. The range of dose values as a function of ThO_2 and UO_2 content in minerals for geological ages of 1 M.y. to 1 G.y. is shown in Fig. 7. Using equation 8 with Th and U contents measured by electron microprobe analysis together with X-ray diffraction to determine the level of radiation damage, Lumpkin and Ewing (1988) demonstrated that the critical dose for amorphization of

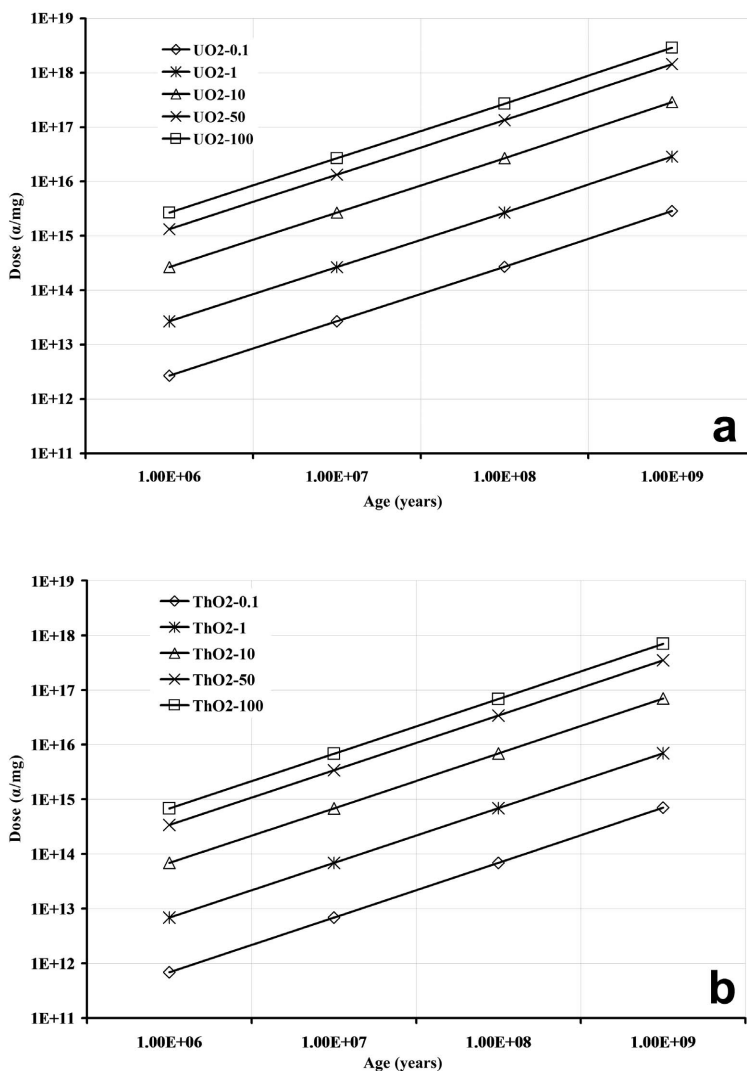


FIG. 7. Alpha-decay dose values for minerals in general as a function of geological age, calculated using equation 8. (a) Dose vs. age for UO_2 content in wt.%, ^{238}U only. (b) Dose vs. age for ThO_2 content in wt.%. Note that natural uraninite and thorianite, based on these calculations, remain crystalline to very large alpha-decay dose values.

natural pyrochlore increases with increasing geological age of the samples. The dose vs. age relationship is described by the equation:

$$D_c = D_0 e^{tK} \tag{9}$$

In this expression, D_0 is the intercept dose and K is a rate constant related to the recovery of radiation damage over time. An example of the effect of varying K on the critical dose for amorphization is shown in Fig. 8. For natural pyrochlores, equation 8 gives $D_0 = 1.4 \times 10^{16} \alpha/\text{mg}$ and $K = 1.7 \times 10^{-9} \text{ y}^{-1}$ for the critical dose (e.g. Lumpkin *et al.*, 1994). The crystalline–amorphous phase transformation of natural pyrochlore was also studied in some detail by Lumpkin and Ewing (1988) using the measured change in Bragg peak intensities by X-ray powder diffraction. The results were evaluated as a function of dose using an equation of the form:

$$I/I_0 = e^{-BD} \tag{10}$$

In equation 10, I/I_0 is the total intensity of all observable Bragg peaks in a given range of the diffraction angle 2θ divided by the total intensity obtained from a highly crystalline reference sample of similar composition and B is a constant related to the amount of material damaged by each alpha-decay event. Analysis of the pyrochlore data yielded $B = 2.6 \times 10^{-16} \text{ mg}/\alpha$, which is equivalent to an average cascade radius of 2.3 nm (Lumpkin and Ewing, 1988). Line broadening was also investigated in these samples,

showing that crystallite dimensions decreased from ~500 to 15 nm with increasing dose. Strain increased initially with dose and reached a maximum of ~0.003 before falling to values below 0.0005 at higher dose levels, consistent with a description of the crystalline–amorphous transformation as a type of ‘percolation’ transition as described by Salje *et al.* (1999).

Early studies of natural zirconolite focussed on the structure and annealing behaviour of samples that were amorphous due to radiation damage. These studies provided evidence that amorphous zirconolite lacks periodicity beyond the second coordination sphere, consistent with a random network model of the amorphous state (e.g. Lumpkin *et al.*, 1986). X-ray absorption spectroscopy indicated that amorphous zirconolite is not periodic beyond the first coordination sphere, with slightly reduced bond lengths, reduced coordination number and increased distortion of the Ti–O polyhedra. Apart from increases in the range of Ca–O, Zr–O and Th–O distances, the local environments of the larger cations do not change much relative to annealed samples (Farges *et al.*, 1993; Farges, 1997). Suites of strongly zoned zirconolite samples from the contact metamorphic rocks of the Bergell intrusion (Switzerland–Italy) and the Adamello igneous complex (Italy) provided the first detailed constraints on the crystalline–amorphous transformation in natural zirconolite (Lumpkin *et al.*, 1997). Analytical electron microscopy, combining energy-

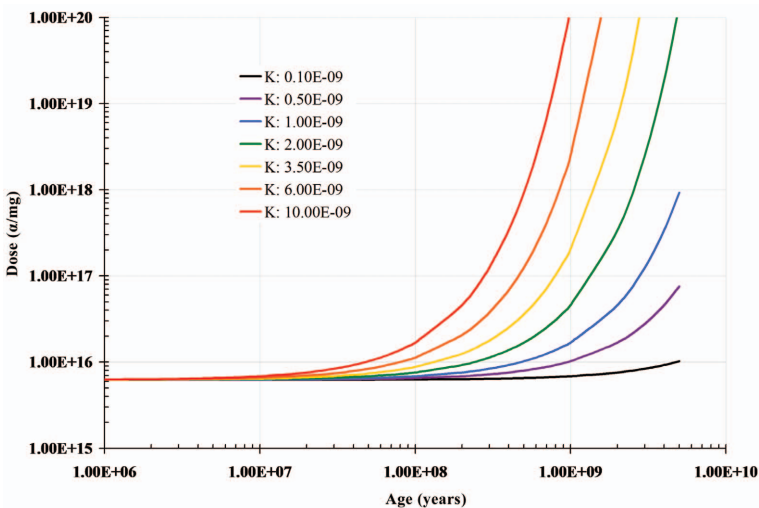


FIG. 8. Effect of variation in the rate constant, K , over two orders of magnitude, calculated using equation 9 with $D_0 = 0.6 \times 10^{16} \alpha/\text{mg}$.

dispersive spectroscopy analysis to obtain the alpha-decay dose with electron diffraction and imaging techniques was used in this study to describe the percolation-like behaviour as a function of dose ranging from $D = 0.08 \times 10^{16}$ α/mg in the highly crystalline (low Th, U) zones to $\sim 0.7\text{--}0.9 \times 10^{16}$ α/mg in the extensively damaged (high Th, U) zones of the μm -scale crystals. Further studies of seven suites of zirconolite samples ranging in age from 16 to 2060 Ma and with alpha-decay doses of $\sim 0.01 \times 10^{16}$ to 24×10^{16} α/mg provided evidence for upward curvature of the onset and critical amorphization dose of natural zirconolite as a function of age. Using equation 9, analysis of this data set returned values of $D_0 = 0.11 \times 10^{16}$ α/mg with $K = 1.0 \times 10^{-9}$ y^{-1} for the onset dose and $D_0 = 0.94 \times 10^{16}$ α/mg with $K = 0.98 \times 10^{-9}$ y^{-1} for the critical dose for amorphization of natural zirconolite (Lumpkin *et al.*, 1998).

Due to the high U content, most natural brannerite samples with ages $\gg 20$ Ma appear to be amorphous (Lumpkin *et al.*, 2000, 2012) due to alpha-decay damage leading to cumulative alpha-decay doses of $2\text{--}170 \times 10^{16}$ α/mg (see Fig 7a). Electron-diffraction patterns of relatively unaltered areas of the brannerite samples consist typically of two broad, diffuse rings characteristic of amorphous materials. An estimate of the critical dose for amorphization is provided by the partially crystalline brannerite from Binntal, Switzerland (Graeser and Guggenheim, 1990). With an age of ~ 10 Ma, this occurrence allows the critical dose to be estimated at $\sim 1 \times 10^{16}$ α/mg , similar to some of the pyrochlore and zirconolite samples with geological ages in this time frame.

Recent work on davidite from several different localities shows that this mineral has experienced cumulative alpha-decay dose levels of $\sim 0.2\text{--}44 \times 10^{16}$ α/mg (Lumpkin *et al.*, 2013). Electron microscopy observations also show that samples with doses $\gg 1 \times 10^{16}$ α/mg have been rendered amorphous; however, one crystalline specimen from Waterford, Connecticut, USA was described with lower levels of ThO_2 (0.1–0.5 wt.%) and UO_2 (0.2–0.7 wt.%), resulting in a maximum cumulative dose of $\sim 0.6 \times 10^{16}$ α/mg . These data provide an approximation for the critical dose for amorphization of $\sim 0.8 \times 10^{16}$ α/mg for the younger samples having ages of $\sim 270\text{--}300$ Ma. Electron-diffraction patterns show that different parts of the Waterford sample range from highly crystalline to partially radiation damaged, compared to the

other samples wherein only diffuse rings are observed. High-resolution transmitted electron microscopy images of thin areas of the partially-damaged grains show amorphous domains within the crystalline matrix, similar to the microstructure observed in pyrochlore, titanite, zircon and zirconolite (Lumpkin and Ewing, 1988; Hawthorne *et al.*, 1991; Lumpkin *et al.*, 1991; Murakami *et al.*, 1991; Lumpkin *et al.*, 1997). Using literature data for other crichtonite-group minerals from Tuscany, Italy and two Norwegian localities, Lumpkin *et al.* (2013) were able to construct an approximate ‘median’ critical dose curve with values of $D_0 = 0.51 \times 10^{16}$ α/mg and $K = 1.5 \times 10^{-9}$ y^{-1} using equation 9.

In-depth studies have not been conducted on radiation damage in natural perovskite; however, Lumpkin *et al.* (1998) examined a suite of samples with ages of 295–520 Ma using analytical electron microscopy and reported ThO_2 contents of 1.4–3.1 wt.% indicating that the beginning of the crystalline–amorphous transformation (e.g. first observable damage, not the critical dose) occurs within the dose range of $0.3\text{--}0.6 \times 10^{16}$ α/mg . With higher ThO_2 contents of up to 6.0 wt.%, perovskite samples from Bratthagen, Norway have experienced cumulative alpha-decay doses up to 1.2×10^{16} α/mg and are partially radiation damaged based on the appearance of a weak diffuse ring in electron-diffraction patterns. Elsewhere, Th-rich perovskites from the Khibina alkaline complex, Russia, have been studied in some detail by Mitchell and Chakhmouradian (1998). These samples are zoned chemically and contain 2.3–18.5 wt.% ThO_2 which increases from the cores to the rims of individual perovskite crystals. X-ray diffraction studies indicate that the cores (2.3–7.4 wt.% ThO_2) are partially crystalline and the rims (8.7–18.5 wt.% ThO_2) are completely amorphous, providing an estimate of the critical dose for amorphization of $\sim 2 \times 10^{16}$ α/mg based on the maximum and minimum Th contents of the cores and rims, respectively.

Radiation damage effects in zircon have been studied extensively due to the importance of the mineral in geological-age determination and as a proposed host phase for Pu in nuclear waste forms. The early classic investigations of natural zircon samples by Hurley and Fairbairn (1953) and Holland and Gottfried (1955) elucidated a transformation from the crystalline to the amorphous state as a function of alpha activity or alpha-decay dose *via* careful examination of

X-ray diffraction patterns, calculation of lattice parameters and measurements of optical properties and density. In particular, measurements of the densities of zircons from Sri Lanka were shown to decrease by ~16% with increasing dose, whilst the unit-cell parameters increased anisotropically up to a dose of $\sim 0.6 \times 10^{16}$ α/mg (Holland and Gottfried, 1955). Much later, a more detailed analysis of the X-ray scattering in zircon samples from Sri Lanka enabled the deconvolution of peaks in the powder patterns into the Bragg and diffuse components, the latter due to the strong influence of radiation-induced defects (e.g. Frenkel pairs) in the lower-dose regime (Murakami *et al.*, 1991). Key features of this work include the accurate determination of anisotropic lattice expansion with increasing dose, unit-cell volume expansion of 4.7% and total volume expansion of ~18%. In a single large zoned crystal of zircon from Sri Lanka, Chakoumakos *et al.* (1991) demonstrated that the hardness and elastic modulus decreased by 40% and 25%, respectively, with increasing alpha-decay dose up to $\sim 1.0 \times 10^{16}$ α/mg .

Other notable studies of natural zircon samples have addressed the energetics of radiation damage as a function of dose and the nano-scale effects of recrystallization of extensively damaged material to phase assemblages consisting of various combinations of zirconia (tetragonal or monoclinic), quartz and silica glass (e.g. Ellsworth *et al.*, 1994; McLaren *et al.*, 1994). Atomistic modelling and experimental work conducted at the University of Cambridge using molecular dynamics simulations and nuclear magnetic resonance spectroscopy revealed that local segregation of Si and Zr occurs within the alpha-recoil collision cascades in zircon, thereby planting the seeds for breakdown of extensively damaged zircon to the phase assemblages noted above during natural annealing over time (Trachenko *et al.*, 2002; Farnan and Salje, 2001). In their detailed examination of radiation effects in zircon, Meldrum *et al.* (1998) proposed a method to relate the equivalent U content and the geological age to the critical temperature for amorphization and activation energy for damage recovery determined by laboratory ion irradiation. Although the method has not been employed widely in studies of radiation damage, the results suggest that the thermal history of the host rocks may play an important role in the level of radiation damage observed in natural zircons. This has been demonstrated quite elegantly in

another important study of zircons from Sri Lanka (Nasdala *et al.*, 2004), including the evaluation of the time–temperature history of the host rocks and its influence on damage recovery in the samples.

In comparison to the oxides and other ABO_4 silicates described above, all natural monazites are found in the crystalline state, even at high dose levels approaching 10^{17} α/mg , a feature that makes synthetic monazite-based materials very attractive for nuclear waste encapsulation. In laboratory studies, the radiation stability of synthetic $(\text{La,Pu})\text{PO}_4$ and PuPO_4 doped with 8.1 and 7.2 wt.% ^{238}Pu , respectively, has been investigated by Burakov *et al.* (2004). These authors discovered that $(\text{La,Pu})\text{PO}_4$ remains crystalline up to a dose of $\sim 0.2\text{--}0.3 \times 10^{16}$ α/mg , albeit with a decrease in the intensity of the measured X-ray diffraction peaks. In contrast to this result, the PuPO_4 ceramic sample is damaged extensively at a dose of only $\sim 0.1 \times 10^{16}$ α/mg and exhibits substantial volume swelling and cracking. Furthermore, laboratory-based ion-irradiation studies (Meldrum *et al.*, 1997) reveal that natural monazite (Ce dominant *Ln* distribution) and synthetic monazites with *Ln* = La–Gd are all amorphized easily, albeit with low critical temperatures for amorphization. Thus, there is an important link between all of these studies related to the kinetics of damage recovery over time.

A summary of the currently known radiation damage response of natural analogues in terms of the critical dose for amorphization vs. geological age is provided in Fig. 9. For the younger host rocks with $t = 1\text{--}10$ M.y., where the curves are relatively flat, the critical dose for amorphization increases in the order zircon < davidite < zirconolite < pyrochlore < brannerite. For geologically older samples, it can be seen that (1) perovskite may have a slightly larger dose than pyrochlore; (2) the order of radiation tolerance may change; and (3) metamorphosed pyrochlore from Blue River, British Columbia, has a significantly larger critical dose compared with unmetamorphosed samples of similar age due to a significantly higher average temperature relative to the unmetamorphosed pyrochlores. The critical dose values of the minerals discussed in this paper are summarized in Table 3 for several different values of geological age, together with the rate constant K obtained from equation 9. For pyrochlore and zirconolite, the observed D_c values for the youngest samples are larger than the critical doses measured in the laboratory using

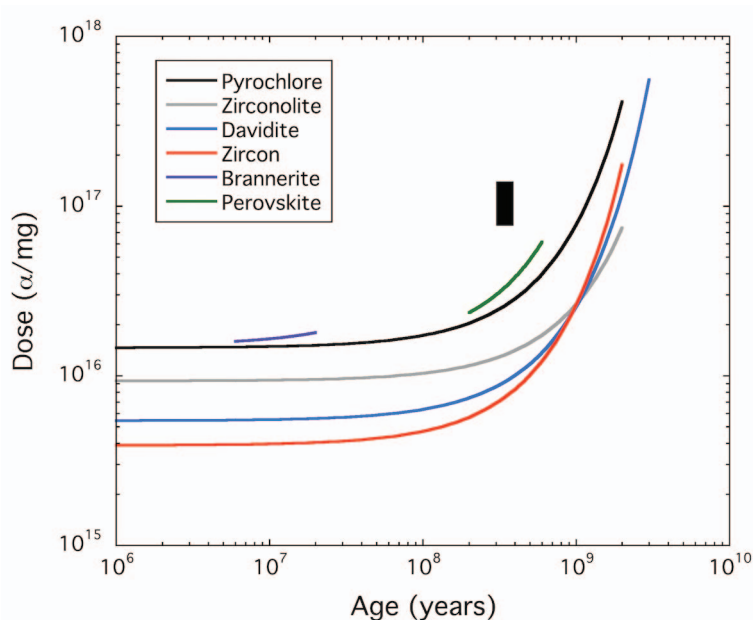


FIG. 9. Summary of dose vs. age data for minerals. Curves showing the critical dose for amorphization vs. geological age are shown for minerals from many localities with sufficient variation in the Th-U content to bracket the critical dose. The zirconolite curve reflects an average temperature on the order of 100–200°C based on the thermal histories of the host rocks. The pyrochlore curve may reflect a similar average temperature, but the thermal histories of some of the samples are less well known. There is much greater uncertainty in the zircon curve due to largely unknown thermal histories and weighting of the data to older samples with $t > 100$ M.y. The black box shows the approximate critical dose range for metamorphosed pyrochlore from Blue River, British Columbia, Canada (see Fig. 1 for thermal history data).

synthetic samples doped with ^{238}Pu or ^{244}Cm (Clinard *et al.*, 1984*a,b*; Weber *et al.*, 1986). These differences are consistent with dose-rate effects, including the storage of the natural samples at an elevated temperature over long periods of time. For zircon, the D_c value obtained

from natural samples appears to be lower than the critical dose found in the short-term laboratory studies *via* ^{238}Pu doping (see Weber *et al.*, 1997). The reason for this discrepancy is not immediately obvious; however, it is noteworthy that the zircon data are dominated by samples with older

TABLE 3. Radiation-damage data for natural analogues, including the critical dose for amorphization for several different geological ages and the rate constant for annealing of damage with time. Note that the zircon data may not accurately reflect significant differences in the thermal histories of the host rocks.

Mineral	— D_c (10^{16} α/mg) at selected age intervals —				K (10^{-9} y^{-1})
	$t = 1$ M.y.	$t = 100$ M.y.	$t = 1$ G.y.	$t = 2$ G.y.	
Pyrochlore	1.3	1.6	8	41	1.7
Metamorphosed pyrochlore			~8–22		n.a.
Zirconolite	0.92	1.0	2.5	7	0.98
Brannerite	~1.6–1.8				n.a.
Davidite	0.57	0.69	2.1	9	1.5
Perovskite			~2–10		~2.3
Zircon	~0.4 ?	~0.5 ?	3.1	27	~2.0 ?

geological ages due to lower Th and U contents, leading to greater uncertainty in the intercept dose. Furthermore, as pointed out by Nasdala *et al.* (2004) the observed level of damage may be quite sensitive to the thermal history of the host rocks and this has not been taken into account here.

Discussion and conclusions

In terms of crystal-chemical flexibility, studies of natural analogues indicate that the pyrochlore structure type is indeed a suitable host for actinides and certain fission products and for processing contaminants, including F, Na, Ca, Zr and light lanthanides. However, the incorporation of F and Na is generally hampered by the bulk compositions and processing methods currently employed for waste form production. Zirconolite also has excellent chemical flexibility for actinides, lanthanides (generally mid-series), Ca, Zr and transition metals (e.g. Cr–Zn). A waste form similar to that designed for the US Plutonium Immobilization Project, containing pyrochlore and zirconolite as major phases, provides a ‘one-two punch’ for a range of HLW elements and continues to be an attractive option for fissile-materials disposal. Even though both structure types are susceptible to amorphization induced by radiation damage, the volume swelling is low (~5 vol.%) and aqueous durability remains acceptable. Zirconolite exhibits very low dissolution rates in aqueous fluids over a range of pH and fluid compositions.

Brannerite appears to be less resistant to alteration for samples with geological ages greater than ~70 Ma and may lose substantial amounts of U and incorporate large amounts of Si into the radiation damaged, glass-like structure. Pyrochlore, zirconolite and brannerite are reported to incorporate Si in the presence of SiO₂-bearing aqueous fluids and this is an important subject for future research. Crichtonite group minerals appear to have some promise as host phases for a range of actinides and fission products, including Sr. However, minerals in this group such as davidite, crichtonite *sensu stricto*, dessaute and lovingite are easily amorphized relative to the other minerals described here. Furthermore, davidite is susceptible to breaking down to mineral assemblages consisting of titanite, ilmenite and rutile, depending upon the local fluid composition. A considerable amount of work is required to understand this mineral group in detail in the context of nuclear waste disposal.

The crystal chemistry of perovskite suggests that it would be an excellent host phase for Na, Sr, certain transition metals and the light lanthanides, but perhaps less suitable for actinides. However, aqueous durability observations coupled with dedicated laboratory studies demonstrate that perovskite is readily dissolved at low to moderate temperatures, reacting with the aqueous medium to produce TiO₂ as an alteration product and releasing Ca, Ln and other elements to the fluid phase. One option for perovskite is short- to medium-term surface deployment as a dedicated host phase for short-lived, heat generating, radioactive ⁹⁰Sr from separated HLW.

Although zircon has been studied extensively, it appears to be less suitable as a waste form due to the low solubility of waste-form elements in the structure, ease of amorphization and propensity for cracking due to anisotropic volume expansion. The actinide orthosilicates, however, are able to overcome some of these limitations. Thorite, for example, provides a high waste loading for actinides, can incorporate higher levels of impurities relative to zircon and has the potential for increased radiation tolerance by tailoring the composition towards compositions with P on the tetrahedral site instead of Si. Monazite continues to be a very attractive option for a range of actinides, fission products such as the light lanthanides and even Sr. Although monazite remains crystalline over geological periods of time, it does not readily accommodate Na, transition metals and Zr.

In closing, we note that Sowder *et al.* (2013), in discussing the need for a geological repository in the United States (and in general), stated that “...there exists today an international consensus on the appropriateness and capability of deep geologic disposal for providing long-term isolation of used fuel and HLW from the biosphere. This consensus has emerged from more than five decades of site selection and characterization, scientific study and peer review and regulatory oversight.” We believe that there is a continued role for the study of natural analogues and their host rocks by earth scientists with a range of modern skills, together with laboratory-based experimental investigations in order to understand the behaviour of nuclear materials in geological repositories. It is approaching 15 years since Ewing (1999) published an article in *Science* entitled “Less geology in the geological disposal of nuclear waste”. Now is the time to begin to reverse that trend.

References

- Banfield, J.F. and Veblen, D.R. (1992) Conversion of perovskite to anatase and TiO_2 (B): A TEM study and the use of fundamental building blocks for understanding relationships among the TiO_2 minerals. *American Mineralogist*, **77**, 545–557.
- Bates, J.K., Ebert, W.L., Feng, X. and Bourcier, W.L. (1992) Issues affecting the prediction of glass reactivity in an unsaturated environment. *Journal of Nuclear Materials*, **190**, 198–227.
- Begg, B.D. (2003) Titanate ceramic matrices for nuclear waste immobilisation. *Research Advances in Ceramics*, **1**, 49–62.
- Boatner, L.A. (2002) Synthesis, structure, and properties of monazite, pretilite, and xenotime, Pp. 87–122 in: *Phosphates: Geochemical, Geobiological, and Materials Importance* (M.J. Kohn, J. Rakovan and J.M. Hughes, editors). Reviews in Mineralogy & Geochemistry, **48**. Mineralogical Society of America, Washington, DC.
- Boatner, L.A. and Sales, B.C. (1988) Monazite. Pp. 495–564 in: *Radioactive Waste Forms for the Future* (W. Lutze and R.C. Ewing, editors). North-Holland, Amsterdam.
- Bulakh, A.G., Nesterov, A.R., Williams, C.T. and Anisimov, I.S. (1998) Zirkelite from the Sebl' yavr carbonatite complex, Kola peninsula, Russia: an X-ray and electron microprobe study of a partially metamict mineral. *Mineralogical Magazine*, **62**, 837–846.
- Burakov, B.E., Yagovkina, M.A., Garbuzov, V.M., Kitsay, A.A. and Zirlin, V.A. (2004) Self-irradiation of monazite ceramics – contrasting behavior of PuPO_4 and $(\text{La},\text{Pu})\text{PO}_4$ doped with Pu-238. Pp. 219–224 in: *Scientific Basis for Nuclear Waste Management XXVIII. Materials Research Society Symposium Proceedings* (J.M. Hanchar, S. Stroes-Gascoyne and L. Browning, editors), **824**. Materials Research Society, Warrendale, Pennsylvania, USA.
- Campbell, I.H. and Kelly, P.R. (1978) The geochemistry of loveringite, a uranium-rare-earth-bearing accessory phase from the Jemberlana Intrusion of Western Australia. *Mineralogical Magazine*, **42**, 187–193.
- Chakhmouradian, A.R. and Mitchell, R.H. (1998) Lueshite, pyrochlore and monazite-(Ce) from apatite-dolomite carbonatite, Lesnaya Varaka complex, Kola Peninsula, Russia. *Mineralogical Magazine*, **62**, 769–782.
- Chakhmouradian, A.R., Mitchell, R.H., Pankov, A.V. and Chukanov, N.V. (1999) Loparite and 'metaloparite' from the Burpala alkaline complex, Baikalk Alkaline Province (Russia). *Mineralogical Magazine*, **63**, 519–534.
- Chakoumakos, B.C. (1984) Systematics of the pyrochlore structure type, ideal $\text{A}_2\text{B}_2\text{X}_6\text{Y}$. *Journal of Solid State Chemistry*, **53**, 120–129.
- Chakoumakos, B.C., Murakami, T., Lumpkin, G.R. and Ewing, R.C. (1987) Alpha-decay induced fracturing in zircon: The transition from the crystalline to the metamict state. *Science*, **236**, 1556–1559.
- Chakoumakos, B.C., Oliver, W.C., Lumpkin, G.R. and Ewing, R.C. (1991) Hardness and elastic modulus of zircon as a function of heavy-particle irradiation dose: I. In situ alpha-decay event damage. *Radiation Effects and Defects in Solids*, **118**, 393–403.
- Clarke, D.R., Jantzen, C.M. and Harker, A.B. (1982) Dissolution of tailored ceramic nuclear waste forms. *Nuclear and Chemical Waste Management*, **3**, 59–66.
- Clinard, F.W., Jr., Peterson, D.E., Rohr, D.L. and Hobbs, L.W. (1984a) Self-irradiation effects in ^{238}Pu -substituted zirconolite, I: temperature dependence of damage. *Journal of Nuclear Materials*, **126**, 245–254.
- Clinard, F.W., Jr., Rohr, D.L. and Roof, R.B. (1984b) Structural damage in a self-irradiated zirconolite-based ceramic. *Nuclear Instruments and Methods in Physics Research B*, **1**, 581–586.
- Cuney, M. and Mathieu, R. (2000) Extreme light rare-earth element mobilisation by diagenetic fluids in the geological environment of the Okla natural reactor zones, Franceville basin, Gabon. *Geology*, **28**, 743–746.
- De Vito, C., Pezzotta, F., Ferrini, V. and Aurisicchio, C. (2006) Nb-Ti-Ta oxides in the gem-mineralized and "hybrid" Anjanabonoina granitic pegmatite, central Madagascar: a record of magmatic and postmagmatic events. *The Canadian Mineralogist*, **44**, 87–103.
- Ellsworth, S., Navrotsky, A. and Ewing, R.C. (1994) Energetics of radiation damage in natural zircon (ZrSiO_4). *Physics and Chemistry of Minerals*, **21**, 140–149.
- Ewing, R.C. (1999) Less geology in the geological disposal of nuclear waste. *Science*, **286**, 415–417.
- Ewing, R.C., Haaker, R.F. and Lutze, W. (1982) Leachability of zircon as a function of alpha dose. Pp. 389–397 in: *Scientific Basis for Nuclear Waste Management V* (W. Lutze, editor). Elsevier, New York.
- Ewing, R.C., Lutze, W. and Webber, W.J. (1995) Zircon: a host-phase for the disposal of weapons plutonium. *Journal of Materials Research*, **10**(2), 243–246.
- Ewing, R.C., Weber, W.J., and Lian, J. (2004) Nuclear waste disposal – pyrochlore ($\text{A}_2\text{B}_2\text{O}_7$): nuclear waste form for the immobilization of plutonium and "minor" actinides. *Journal of Applied Physics*, **95**, 5949–5971.
- Farges, F. (1997) Five fold-coordinated Ti^{4+} in metamict zirconolite and titanite: a new occurrence shown by Ti K-edge XANES spectroscopy. *American*

- Mineralogist*, **82**, 44–50.
- Farges, F., Ewing, R.C. and Brown, G.E. (1993) The structure of aperiodic, metamict $(\text{Ca,Th})\text{ZrTi}_2\text{O}_7$ (zirconolite): an EXAFS study of the Zr, Th, and U sites. *Journal of Materials Research*, **8**, 1983–1995.
- Farnan, I. and Salje, K.H. (2001) The degree and nature of radiation damage in zircon observed by ^{29}Si nuclear magnetic resonance. *Journal of Applied Physics*, **89**, 2084–2090.
- Förster, H.J. (1998) The chemical composition of REE-Y-Th-U-rich accessory minerals in peraluminous granites of the Erzgebirge-Fichtelgebirge region, Germany, Part I: The monazite-(Ce)-brabantite solid solution series. *American Mineralogist*, **83**, 259–272.
- Forsyth, R.S. and Werme, L.O. (1992) Spent fuel corrosion and dissolution. *Journal of Nuclear Materials*, **190**, 3–19.
- Fron del, C. (1958) Systematic mineralogy of uranium and thorium. *U.S. Geological Survey Bulletin*, **1064**, 400.
- Gatehouse, B.M., Grey, I.E., Campbell, I.H. and Kelly, P.R. (1978) The crystal structure of lovingite – a new member of the crichtonite group. *American Mineralogist*, **63**, 28–36.
- Gatehouse, B.M., Grey, I.E. and Kelly, P.R. (1979) The crystal structure of davidite. *American Mineralogist*, **64**, 1010–1017.
- Geisler, T., Ulonska, M., Schleicher, H., Pidgeon, R.T. and van Bronswijk, W. (2001) Leaching and differential recrystallization of metamict zircon under experimental hydrothermal conditions. *Contributions to Mineralogy and Petrology*, **141**, 53–65.
- Geisler, T., Rashwan, A.A., Rahn, M., Poller, U., Zwingmann, H., Pidgeon, R.T., Schleicher, H. and Tomaschek, F. (2003) Low-temperature hydrothermal alteration of natural metamict zircons from the Eastern Desert, Egypt. *Mineralogical Magazine*, **67**, 485–508.
- Gieré, R., Williams, C.T. and Lumpkin, G.R. (1998) Chemical characteristics of natural zirconolite. *Schweizerische Mineralogische und Petrographische Mitteilungen*, **78**, 433–459.
- Gieré, R., Buck, E.C., Guggenheim, R., Mathys, D., Reusser, E. and Marques, J. (2001) Alteration of Uranium-rich microlite. Pp. 935–944 in: *Scientific Basis for Nuclear Waste Management XXIV. Materials Research Society Symposium Proceedings* (K.P. Hart and G.R. Lumpkin, editors), **663**. Materials Research Society, Warrendale, Pennsylvania, USA.
- Gong, W.L., Ewing, R.C., Wang, L.M. and Xie, H.S. (1995) Crichtonite structure type ($\text{AM}_{21}\text{O}_{38}$ and $\text{A}_2\text{M}_{19}\text{O}_{36}$) as a host phase in crystalline waste form ceramics. *Materials Research Society Symposium Proceedings*, **353**, 807–815.
- Graeser, S. and Guggenheim, R. (1990) Brannerite from Lengenbach, Binntal (Switzerland). *Schweizerische Mineralogische und Petrographische Mitteilungen*, **70**, 325–331.
- Grambow, B. (1994) Borosilicate glass: Future research requirements or “What we don’t know”. *MRS Bulletin*, **XIX(12)**, 20–23.
- Grey, I.E. and Gatehouse, I.E. (1978) The crystal structure of landauite, $\text{Na}[\text{MnZn}_2(\text{Ti,Fe})_6\text{Ti}_{12}]\text{O}_{38}$. *The Canadian Mineralogist*, **16**, 63–68.
- Grey, I.E., Lloyd, D.J. and White, J.S., Jr. (1976) The structure of crichtonite and its relationship to senaite. *American Mineralogist*, **61**, 1203–1212.
- Hansmann, W. (1996) Age determinations on the Tertiary Masino–Bregaglia (Bergell) intrusives (Italy, Switzerland): a review. *Schweizerische Mineralogische und Petrographische Mitteilungen*, **76**, 421–451.
- Harker, A.B. (1988) Tailored ceramics. Pp. 335–392 in: *Radioactive Waste Forms for the Future*. (W. Lutze and R.C. Ewing, editors). North-Holland, Amsterdam.
- Hart, K.P., Lumpkin, G.R., Gieré, R., Williams, C.T., McGlenn, P.J. and Payne, T.E. (1996) Naturally occurring zirconolites – analogues for the long-term encapsulation of actinides in Synroc. *Radiochimica Acta*, **74**, 309–312.
- Hawthorne, F.C., Groat, L.A., Raudsepp, M., Ball, N.A., Kimata, M., Spike, F.D., Gaba, R., Halden, N.M., Lumpkin, G.R., Ewing, R.C., Gregor, R.B., Lytle, F.W., Ercit, T.S., Rossman, G.R., Wicks, F.J., Ramik, R.A., Sherriff, B.L., Fleet, M.E. and McCammon, C. (1991) Alpha-decay damage in titanite. *American Mineralogist*, **76**, 370–396.
- Hecht, L. and Cuney, M. (2000) Hydrothermal alteration of monazite in the Precambrian crystalline basement of the Athabasca Basin (Saskatchewan, Canada): Implications for the formation of unconformity-related uranium deposits. *Mineralium Deposita*, **35**, 791–795.
- Hetherington, C.J. and Harlov, D.E. (2008) Metasomatic thorite and uraninite inclusions in xenotime and monazite from granitic pegmatites, Hidra anorthosite massif, southwestern Norway: mechanics and fluid chemistry. *American Mineralogist*, **93**, 806–820.
- Holland, H.D. and Gottfried, D. (1955) The effect of nuclear radiation on the structure of zircon. *Acta Crystallographica*, **8**, 291–300.
- Hurley, P.M. and Fairbairn, H.W. (1953) Radiation damage in zircon: a possible age method. *Geological Society of America Bulletin*, **64**, 659–674.
- Icenhower, J.P., Strachan, D.M., McGrail, B.P., Scheele, R.D., Rodriguez, E.A., Steele, J.L. and Legore, V.L. (2006) Dissolution kinetics of pyrochlore ceramics for the disposition of plutonium. *American*

- Mineralogist*, **91**, 39–53.
- Isobe, H., Murakami, T. and Ewing, R.C. (1992) Alteration of uranium minerals in the Koongarra deposit, Australia: Unweathered zone. *Journal of Nuclear Materials*, **190**, 174–187.
- Janeczek, J. and Ewing, R.C. (1992) Structural formula of uraninite. *Journal of Nuclear Materials*, **190**, 128–132.
- Jensen, M., Lam, T., Luhowy, D., McLay, J., Semec, B. and Frizzell, R. (2009) Overview of Ontario power generation's proposed L&ILW deep geologic repository Bruce site, Tiverton, Ontario. Pp. 149–150 in: *Proceedings of the 3rd Canus Rock Mechanics Symposium* (M. Diederichs and G. Grasselli, editors). Toronto, Canada.
- Johnson, L.H. and Werme, L.O. (1994) Materials characteristics and dissolution behaviour of spent nuclear fuel. *MRS Bulletin*, **XIX(12)**, 24–27.
- King, F., Ahonen, L., Taxén, C., Vuorinen, U. and Werme, L. (2002) *Copper Corrosion Under Expected Conditions in a Deep Geologic Repository*. Report POSIVA 2002-01, Posiva Oy, Helsinki, 184 pp.
- Kynicky, J., Smith, M.P. and Xu, C. (2012) Diversity of rare earth deposits: The key example of China. *Elements*, **8**, 361–367.
- Lumpkin, G.R. (1989) *Alpha-decay damage, geochemical alteration, and crystal chemistry of natural pyrochlores*. Unpublished PhD Dissertation, University of New Mexico, USA.
- Lumpkin, G.R. (1999) Physical and chemical characteristics of baddeleyite (monoclinic zirconia) in natural environments: an overview and case study. *Journal of Nuclear Materials*, **274**, 206–217.
- Lumpkin, G.R. (2001) Alpha-decay damage and aqueous durability of actinide host phases in natural systems. *Journal of Nuclear Materials*, **289**, 136–166.
- Lumpkin, G.R. (2006) Ceramic waste forms for actinides. *Elements*, **2**, 365–372.
- Lumpkin, G.R. and Chakoumakos, B.C. (1988) Chemistry and radiation effects of thorite group minerals from the Harding pegmatite, Taos County, New Mexico. *American Mineralogist*, **73**, 1405–1419.
- Lumpkin, G.R. and Ewing, R.C. (1988) Alpha-decay damage in minerals of the pyrochlore group. *Physics and Chemistry of Minerals*, **16**, 2–20.
- Lumpkin, G.R. and Ewing, R.C. (1992) Geochemical alteration of pyrochlore group minerals: Microlite subgroup. *American Mineralogist*, **77**, 179–188.
- Lumpkin, G.R. and Ewing, R.C. (1995) Geochemical alteration of pyrochlore group minerals: pyrochlore subgroup. *American Mineralogist*, **80**, 732–743.
- Lumpkin, G.R. and Ewing, R.C. (1996) Geochemical alteration of pyrochlore group minerals: Betafite subgroup. *American Mineralogist*, **81**, 1237–1248.
- Lumpkin, G.R. and Geisler-Wierwille, T. (2012) Minerals and natural analogues. Pp. 563–600 in: *Comprehensive Nuclear Materials*, **5** (R.J.M. Konings, editor). Elsevier, Amsterdam.
- Lumpkin, G.R. and Mariano, A.N. (1996) Natural occurrence and stability of pyrochlore in carbonates, related hydrothermal systems, and weathering environments. Pp. 831–838 in: *Scientific Basis for Nuclear Waste Management XIX. Materials Research Society Symposium Proceedings* (W.M. Murphy and D.A. Knecht, editors). **412**. Materials Research Society, Warrendale, Pennsylvania, USA.
- Lumpkin, G.R., Chakoumakos, B.C. and Ewing, R.C. (1986) Mineralogy and radiation effects of microlite from the Harding pegmatite, Taos County, New Mexico. *American Mineralogist*, **71**, 569–588.
- Lumpkin, G.R., Smith, K.L. and Blackford, M.G. (1991) Electron microscope study of Synroc before and after exposure to aqueous solutions. *Journal of Materials Research*, **6**, 2218–2233.
- Lumpkin, G.R., Hart, K.P., McGlenn, P.J., Payne, T.E., Gieré, R. and Williams, C.T. (1994) Retention of actinides in natural pyrochlore and zirconolites. *Radiochimica Acta*, **66/67**, 469–474.
- Lumpkin, G.R., Smith, K.L. and Blackford, M.G. (1995) Partitioning of uranium and rare earth elements in Synroc: effect of impurities, metal additive, and waste loading. *Journal of Nuclear Materials*, **224**, 31–42.
- Lumpkin, G.R., Smith, K.L. and Gieré, R. (1997) Application of analytical electron microscopy to the study of radiation damage in the complex oxide mineral zirconolite. *Micron*, **28**, 57–68.
- Lumpkin, G.R., Colella, M., Smith, K.L., Mitchell, R.H. and Larsen, A.O. (1998) Chemical composition, geochemical alteration, and radiation effects in natural perovskite. Pp. 207–214 in: *Scientific Basis for Nuclear Waste Management XXI. Materials Research Society Symposium Proceedings* (I.G. McKinley and C. McCombie, editors), **506**. Materials Research Society, Warrendale, Pennsylvania, USA.
- Lumpkin, G.R., Day, R.A., McGlenn, P.J., Payne, T.E., Gieré, R. and Williams, C.T. (1999) Investigation of the long-term performance of betafite and zirconolite hydrothermal veins from Adamello, Italy. Pp. 793–800 in: *Scientific Basis for Nuclear Waste Management XXII. Materials Research Society Symposium Proceedings* (D.J. Wronkiewicz and J.H. Lee, editors), **556**. Materials Research Society, Warrendale, Pennsylvania, USA.
- Lumpkin, G.R., Leung, S.H.F. and Colella, M. (2000) Composition, geochemical alteration, and alpha-decay damage effects of natural brannerite. Pp. 55–68 in: *Scientific Basis for Nuclear Waste*

- Management XXIII. Materials Research Society Symposium Proceedings* (R.W. Smith and D.W. Shoosmith, editors). **608**. Materials Research Society, Warrendale, Pennsylvania, USA.
- Lumpkin, G.R., Smith, K.L., Gieré, R. and Williams, C.T. (2004) Geochemical behaviors of host phases for actinides and fission products in crystalline ceramic nuclear waste forms. Pp. 89–111 in: *Energy, Waste, and the Environment: a Geochemical Perspective* (R. Gieré and P. Stille, editors). Special Publications, **236**. Geological Society, London.
- Lumpkin, G.R., Leung, S.H.F. and Ferenzy, J. (2012) Chemistry, microstructure, and alpha decay damage of natural brannerite. *Chemical Geology*, **291**, 55–68.
- Lumpkin, G.R., Blackford, M.G. and Colella, M. (2013) Chemistry and radiation effects of davidite. *American Mineralogist*, **98**, 275–278.
- Mariano, A.N. (1989) Economic geology of rare earth minerals. Pp. 309–337 in: *Geochemistry and Mineralogy of Rare Earth Elements* (B.R. Lipin and G.A. McKay, editors). Reviews in Mineralogy, **21**. Mineralogical Society of America, Washington DC.
- Mathieu, R., Zetterström, L., Cuney, M., Gauthier-Lafaye, F. and Hidaka, H. (2001) Alteration of monazite and zircon and lead migration as geochemical tracers of fluid paleocirculations around the Oklo-Okélobondo and Bangombé natural nuclear reaction zones (Franceville basin, Gabon). *Chemical Geology*, **171**, 147–171.
- McCarthy, G.J. (1976) High-level waste ceramics. *Transactions of the American Nuclear Society*, **23**, 168–169.
- McCarthy, G.J. (1977) High-level waste ceramics: materials considerations and product characterization. *Nuclear Technology*, **32**, 92–104.
- McLaren, A.C., Fitzgerald, J.D. and Williams, I.S. (1994) The microstructure of zircon and its influence on the age determination from Pb/U isotopic ratios measured by ion microscope. *Geochimica et Cosmochimica Acta*, **58**, 993–1005.
- Meldrum, A., Boatner, L.A. and Ewing, R.C. (1997) Displacive radiation effects in the monazite- and zircon-structure orthophosphates. *Physical Review B*, **56**, 13805–13814.
- Meldrum, A., Boatner, L.A., Weber, W.J. and Ewing, R.C. (1998) Radiation damage in zircon and monazite. *Geochimica et Cosmochimica Acta*, **62(14)**, 2509–2520.
- Mitchell, R.H. (2002) *Perovskites Modern and Ancient*. Almaz Press, Thunder Bay, Ontario, Canada.
- Mitchell, R.H. and Chakhmouradian, A.R. (1998) Th-rich loparite from the Khibina alkaline complex, Kola Peninsula: isomorphism and paragenesis. *Mineralogical Magazine*, **62**, 341–353.
- Mitchell, R.H., Wu, F.-Y., and Yang, Y.-H. (2011) In situ U-Pb, Sr and Nd isotopic analysis of loparite by LA-(MC)-ICP-MS. *Chemical Geology*, **280**, 190–199.
- Murakami, T., Chakoumakos, B.C., Ewing, R.C., Lumpkin, G.R. and Weber, W.J. (1991) Alpha-decay event damage in zircon. *American Mineralogist*, **76**, 1510–1532.
- Nasdala, L., Reiners, P.W., Garver, J.I., Kennedy, A.K., Stern, R.A., Balan, E. and Wirth, R. (2004) Incomplete retention of radiation damage in zircon from Sri Lanka. *American Mineralogist*, **89**, 219–231.
- Nasraoui, M., Bilal, E., and Gibert, R. (1999) Fresh and weathered pyrochlore studies by Fourier transform infrared spectroscopy coupled with thermal analysis. *Mineralogical Magazine*, **63**, 567–578.
- Nesbitt, H.W., Bancroft, G.M., Fyfe, W.S., Karkhanis, S.N. and Nishijima, A. (1981) Thermodynamic stability and kinetics of perovskite dissolution. *Nature*, **289**, 358–362.
- Oelkers, E.H. and Poitrasson, F. (2002) An experimental study of the dissolution stoichiometry and rates of a natural monazite as a function of temperature from 50 to 230°C and pH from 1.5 to 10. *Chemical Geology*, **191**, 73–87.
- Ohnenstetter, D. and Piantone, P. (1992) Pyrochlore-group minerals in the Beauvoir peraluminous leucogranite, Massif Central, France. *The Canadian Mineralogist*, **30**, 771–784.
- Ondrejka, M., Uher, P., Putiš, M., Broska, I., Bačík, P., Konečný, P., and Schmiedt, I. (2012) Two-stage breakdown of monazite by post-magmatic and metamorphic fluids: an example from the Veporic orthogneiss, Western Carpathians, Slovakia. *Lithos*, **142–143**, 245–255.
- Orlandi, P., Pasero, M., Duchi, G. and Olmi, F. (1997) Dessauite, (Sr,Pb)(Y,U)(Ti,Fe³⁺)₂₀O₃₈, a new mineral of the crichtomite group from Buca della Vena mine, Tuscany, Italy. *American Mineralogist*, **82**, 807–811.
- Oversby, V.M. and Phinney, D.L. (1992) The development of surface alteration layers on SRL-165 nuclear waste glasses. *Journal of Nuclear Materials*, **190**, 247–268.
- Oversby, V.M. and Ringwood, A.E. (1981) Lead isotopic studies of zirconolite and perovskite and their implications for long range synroc stability. *Radioactive Waste Management*, **1**, 289–307.
- Poitrasson, F., Chenery, S. and Bland, D.J. (1996) Contrasted monazite hydrothermal alteration mechanisms and their geochemical implications. *Earth and Planetary Science Letters*, **145**, 79–96.
- Poitrasson, F., Chenery, S. and Shepherd, T.J. (2000) Electron microprobe and LA-ICP-MS study of

- monazite hydrothermal alteration: implications for U-Th-Pb geochronology and nuclear ceramics. *Geochimica et Cosmochimica Acta*, **64**, 3283–3297.
- Pršek, J., Ondrejka, M., Bačík, P., Budzyń, B. and Uher, P. (2010) Metamorphic-hydrothermal REE minerals in the Bacúch magnetite deposit, western Carpathians, Slovakia: (Sr,S)-rich monazite-(Ce) and Nd-dominant hingganite. *The Canadian Mineralogist*, **48**, 81–94.
- Rasmussen, B. and Fletcher, I.R. (2004) Zirconolite: a new U-Pb chronometer for mafic igneous rocks. *Geology*, **32**, 785–788.
- Read, D., Andreoli, M.A.G., Knoper, M., Williams, C.T. and Jarvis, N. (2002) The degradation of monazite: Implications for the mobility of rare-earth and actinide elements during low-temperature alteration. *European Journal of Mineralogy*, **14**, 487–498.
- Ringwood, A.E. (1978) *Safe Disposal of High Level Nuclear Reactor Wastes: A New Strategy*, Australian National University Press, Canberra, Australia.
- Ringwood, A.E., Kesson, S.E., Reeve, K.D., Levins, D.M. and Ramm, E.J. (1988) Synroc. Pp. 233–234 in: *Radioactive Waste Forms for the Future* (W. Lutze and R.C. Ewing, editors). North-Holland, Amsterdam.
- Ringwood, A.E., Kesson, S.E., Ware, N.G., Hibberson, W. and Major, A. (1979) Geological immobilisation of nuclear reactor wastes. *Nature*, **278**, 219–223.
- Ringwood, A.E., Oversby, V.M., Kesson, S.E., Sinclair, W., Ware, N., Hibberson, W. and Major, A. (1981) Immobilization of high-level nuclear reactor wastes in synroc: a current appraisal. *Nuclear and Chemical Waste Management*, **2**, 287–305.
- Roberts, S.K., Bourcier, W.L. and Shaw, H.F. (2000) Aqueous dissolution kinetics of pyrochlore, zirconolite and brannerite at 25, 50, and 75°C. *Radiochimica Acta*, **88**, 539–543.
- Salje, E.K.H., Chrosch, J. and Ewing, R.C. (1999) Is “metamictization” of zircon a phase transition? *American Mineralogist*, **84**, 1107–1116.
- Shoesmith, D.W. and Sunder, S. (1992) The prediction of nuclear fuel (UO₂) dissolution rates under waste disposal conditions. *Journal of Nuclear Materials*, **190**, 20–35.
- Smith, K.L., Lumpkin, G.R., Blackford, M.G., Day, R.A. and Hart, K.P. (1992) The durability of Synroc. *Journal of Materials Research*, **190**, 287–294.
- Sowder, A., Kessler, J., Apted, M. and Kozak, M. (2013) What now for permanent disposal of used nuclear fuel and HLW in the United States? *Radwaste Solutions*, **20**, 26–39.
- Staatz, M.H., Adams, J.W. and Wahlberg, J.S. (1976) Brown, yellow, orange, and greenish-black thorites from the Serie pegmatite, Colorado. *Journal of Research of the U.S. Geological Survey*, **4**, 575–582.
- Stefanovsky, S.V., Yudinsev, S.V., Gieré, R. and Lumpkin, G.R. (2004) Nuclear waste forms. Pp. 36–63 in: *Energy, Waste, and the Environment: a Geochemical Perspective* (R. Gieré and P. Stille, editors). Special Publications, **236**. Geological Society, London.
- Strachan, D.M., Scheele, R.D., Buck, E.C., Kozelisky, A.E., Sell, R.L., Elovich, R.J. and Buchmiller, W.C. (2005) Radiation damage effects in candidate titanates for Pu disposition: pyrochlore. *Journal of Nuclear Materials*, **345**, 109–135.
- Subramanian, M.A., Aravamudan, G. and Subba Rao, G.V. (1983) Oxide pyrochlore – a review. *Progress in Solid State Chemistry*, **15**, 55–143.
- Thomas, B.S. and Zhang, Y. (2003) A kinetic model of the oxidative dissolution of brannerite, UTi₂O₆. *Radiochimica Acta*, **91**, 463–472.
- Townsend, K.J., Miller, C.G., D’Andrea, J.L., Ayers, J.C., Harrison, T.M. and Coath, C.D. (2000) Low temperature replacement of monazite in the Ireteba granite, Southern Nevada: geochronological implications. *Chemical Geology*, **172**, 95–112.
- Trachenko, K., Dove, M.T. and Salje, E.K.H. (2002) Structural changes in zircon under α -decay irradiation. *Physical Review B*, **65**, 180102(R).
- Trotignon, L., Petit, J.-C., Della Mea, G. and Dran, J.-C. (1992) The compared aqueous corrosion of four simple borosilicate glasses: Influence of Al, Ca and Fe on the formation and nature of secondary phases. *Journal of Nuclear Materials*, **190**, 228–246.
- Vance, E.R. (1994) Synroc: a suitable waste form for actinides. *Materials Research Society Bulletin*, **XIX**, 28–32.
- Vance, E.R. (2012) Ceramic waste forms. Pp. 485–503 in: *Comprehensive Nuclear Material*, **5** (R.J.M. Konings, editor). Elsevier, Amsterdam.
- Vance, E.R., Lumpkin, G.R., Carter, M.L., Cassidy, D.J., Ball, C.J., Day, R.A. and Begg, B.D. (2002) Incorporation of uranium in zirconolite (CaZr₂O₇). *Journal of American Ceramic Society*, **85**, 1853–1859.
- Wall, F., Williams, C.T. and Woolley, A.R. (1999). Pyrochlore in niobium ore deposits. Pp. 687–690 in: *Mineral Deposits: Processes to Processing* (C.J. Stanley, editor), **1**. Balkema Publishers, Rotterdam.
- Wall, F., Williams, C.T., Woolley, A.R. and Nasraoui, M. (1996) Pyrochlore from weathered carbonatite at Lueshe, Zaire. *Mineralogical Magazine*, **60**, 731–750.
- Weber, W.J., Wald, J.W. and Matzke, H.J. (1986) Effects of self-radiation damage in Cm-doped Gd₂Ti₂O₇ and CaZrTi₂O₇. *Journal of Nuclear Materials*, **138**, 196–209.
- Weber, W.J., Ewing, R.C., and Meldrum, A. (1997) The kinetics of alpha-decay-induced amorphization in zircon and apatite containing weapons-grade plutonium or other actinides. *Journal of Nuclear Materials*, **250**, 147–155.

ROLE OF Th-U MINERALS IN ASSESSING NUCLEAR WASTE FORMS

- Weber, W.J., Ewing, R.C., Catlow, C.R.A., Diaz de la Rubia, T., Hobbs, L.W., Kinoshita, C., Matzke, H.J., Motta, A.T., Nastasi, M., Salje, E.K.H., Vance, E.R. and Zinkle, S.J. (1998) Radiation effects in crystalline ceramics for the immobilization of high-level nuclear waste and plutonium. *Journal of Materials Research*, **13**, 1434–1484.
- Weber, W.J., Navrotsky, A., Stefanovsky, S., Vance, E.R. and Vernaz, E. (2009) Materials science of high-level nuclear waste immobilization. *MRS Bulletin*, **34(1)**, 46–53.
- Williams, C.T. and Gieré, R. (1996) Zirconolite: a review of localities worldwide, and a compilation of its chemical compositions. *Bulletin of the Natural History Museum of London (Geology)*, **52(1)**, 1–24.
- Williams, C.T., Bulakh, A.G., Gieré, R., Lumpkin, G.R. and Mariano, A.N. (2001) Alteration features in natural zirconolites from carbonatites. Pp. 945–952 in: *Scientific Basis for Nuclear Waste Management XXIV. Materials Research Society Symposium Proceedings* (K.P. Hart and G.R. Lumpkin, editors), **663**. Materials Research Society, Warrendale, Pennsylvania, USA.
- Williams, C.T., Wall, F., Wooley, A.R. and Phillipps, S. (1997) Compositional variation in pyrochlore from the Bingo carbonatite, Zaire. *Journal of African Earth Science*, **25**, 137–145.
- Wise, M.A. and Černý, P. (1990) Primary compositional range and alteration trends of microlite from the Yellowknife pegmatite field, Northwest Territories, Canada. *Mineralogy and Petrology*, **43**, 83–98.
- Zhang, Y., Hart, K.P., Bourcier, W.L., Day, R.A., Colella, M., Thomas, B., Aly, Z. and Jostsons, A. (2001) Kinetics of uranium release from Synroc phases. *Journal of Nuclear Materials*, **289**, 254–262.
- Zhang, Y., Thomas, B.S., Lumpkin, G.R., Blackford, M., Zhang, Z., Colella, M. and Aly, Z. (2003) Dissolution of synthetic brannerite in acidic and alkaline fluids. *Journal of Nuclear Materials*, **321**, 1–7.
- Zhang, Z., Blackford, M.G., Lumpkin, G.R., Smith, K.L. and Vance, E.R. (2005) Aqueous dissolution of perovskite (CaTiO₃): Effects of surface damage and [Ca²⁺] in the leachant. *Journal of Materials Research*, **20**, 2462–2473.

